FINAL REPORT

FHWA-WY-17/03F

State of Wyoming
Department of Transportation

US Department of Transportation
Federal Highway Administration

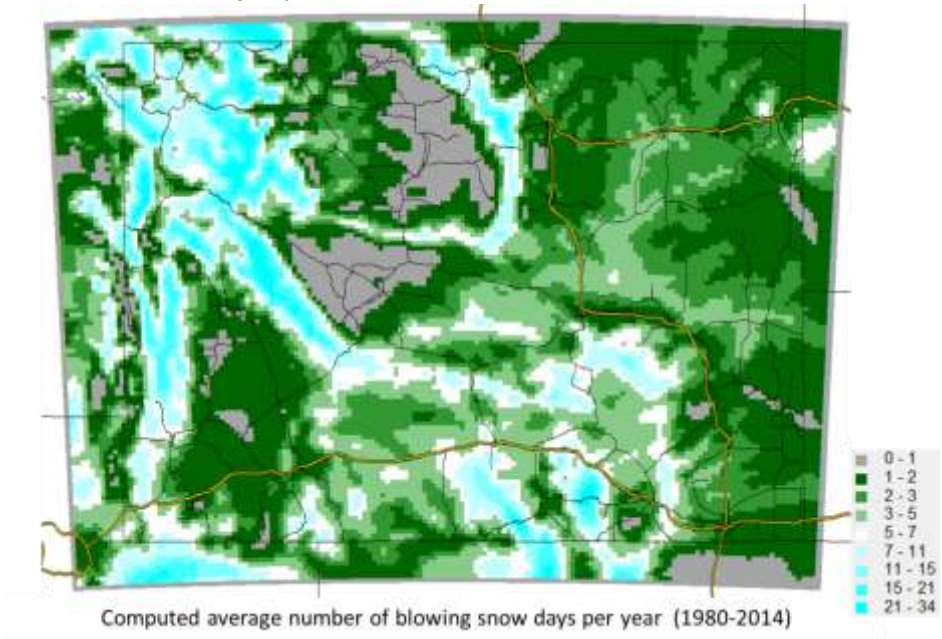

Computed average number of blowing snow days per year (1980-2014)

# HISTORICAL WINTER WEATHER ASSESSMENT FOR SNOW FENCE DESIGN USING A NUMERICAL WEATHER MODEL

By:
Noriaki Ohara, Ph.D., Assistant Professor
Department of Civil and Architectural Engineering
University of Wyoming
1000 E. University Avenue, Dept. 3295
Laramie, Wyoming 82071
Tel: 307.766.4366 | Fax: 307.766.2221
e-mail: nohara1@uwyo.edu

March 30, 2017

## Foreword

This report provides the full technical documentation of the model-based winter weather data for snow fence system in the State of Wyoming. It includes the comparisons to the existing databases, spatial visualizations, the trend analyses of the blowing snow occurrences, the specifications of the data, and the recommendations.

Noriaki Ohara, Ph.D., Assistant Professor
Department of Civil and Architectural Engineering
University of Wyoming
1000 E. University Avenue, Dept. 3295
Laramie, Wyoming 82071

## Disclaimer Notice:

This document is disseminated under the sponsorship of the U.S. Department of Transportation and the Wyoming Department of Transportation in the interest of information exchange. The U.S. Government assumes no liability for the use of the information contained in this document.

The U.S. Government does not endorse products or manufacturers. Trademarks or manufacturers' names appear in this report only because they are considered essential to the objective of the document.



## Quality Assurance Statement:

The Federal Highway Administration (FHWA) provides high-quality information to serve Government, industry, and the public in a manner that promotes public understanding. Standards and policies are used to ensure and maximize the quality, objectivity, utility, and integrity of its information. FHWA periodically reviews quality issues and adjusts its programs and processes to ensure continuous quality improvement.

## Technical Report Documentation Page

| | | | |
|---|---|---|---|
| 1. Report No.<br>FHWA-WY-17/03 | 2. Government Accession No. | 3. Recipient's Catalog No. | |
| 4. Title and Subtitle<br>Historical Winter Weather Assessment for Snow Fence Design using a Numerical Weather Model | | 5. Report Date<br>February 2017 | |
| | | 6. Performing Organization Code | |
| 7. Author(s)<br>Noriaki Ohara, Ph.D., Assistant Professor (0000-0002-7829-0779) | | 8. Performing Organization Report No. | |
| 9. Performing Organization Name and Address<br>University of Wyoming<br>1000 East University Avenue, Dept. 3295<br>Laramie, WY 82070 | | 10. Work Unit No. | |
| | | 11. Contract or Grant No.<br>RS06215 | |
| 12. Sponsoring Agency Name and Address<br>Federal Highway Administration (FHWA) Funded Study<br>Wyoming Department of Transportation (WYDOT)<br>5300 Bishop Blvd.<br>Cheyenne, Wyoming 82001 | | 13. Type of Report and Period Covered<br>Final Report | |
| | | 14. Sponsoring Agency Code<br>FHWA & WYDOT | |
| 15. Supplementary Notes *The data processing software developed in this project is Windstat5 (©2015-2017 Noriaki Ohara) | | | |
| 16. Abstract<br>Snow fence is an effective hazard mitigation measure for the low visibility and low friction of the road surface under winter weather condition. Prevailing wind directions and snow precipitation data prepared by Dr. R. Tabler (the Tabler data) that are necessary for snow fence design have not been updated since the 1990s. This project provides new, seamless wind field and snow precipitation data under the adverse winter storm conditions during 1980-2014, using the Weather Research and Forecasting (WRF) model with North American Regional Reanalysis (NARR) data input. The simulated wind fields were successfully validated by using the observed data from airport sites and using the Tabler data. The WRF simulated precipitation data were assimilated to the observation-based PRISM data in order to obtain the accurate hourly snow precipitation data. Combining all the weather variables, the number of blowing snow events is found to be increasing despite the increasing air temperature because of the sufficiently cold winters of Wyoming. Finally, it was verified that the existing snow fence system is effective under the winter season prevailing wind since the simulation agrees with the Tabler data. However, it was also found that the simulated wind patterns during the blowing snow events can be quite different from the winter season average prevailing wind field. Moreover, the historical wind statistics indicated large deviations in wind direction along I-80. | | | |
| 17. Key Words<br>Snow Fence, Winter Weather, Prevailing Wind Directions, Snow Precipitation, Tabler, Wind Field, Weather Research and Forecasting (WRF), North American Regional Reanalysis (NARR), observation based PRISM data, Wyoming | 18. Distribution Statement<br>This document is available through the National Transportation Library and the Wyoming State Library. Copyright ©2015-17. All rights reserved, State of Wyoming, Wyoming Department of Transportation, and University of Wyoming. All information used which comes from the Tabler Report is copyrighted under ©1997, Ronald D. Tabler. All rights reserved. | | |
| 19. Security Classif. (of this report)<br>Unclassified | 20. Security Classif. (of this page)<br>Unclassified | 21. No. of Pages<br>61 | 22. Price |

## SI* (MODERN METRIC) CONVERSION FACTORS

### APPROXIMATE CONVERSIONS TO SI UNITS

| Symbol | When You Know | Multiply By | To Find | Symbol |
|---|---|---|---|---|
| | | **LENGTH** | | |
| in | inches | 25.4 | millimeters | mm |
| ft | feet | 0.305 | meters | m |
| yd | yards | 0.914 | meters | m |
| mi | miles | 1.61 | kilometers | km |
| | | **AREA** | | |
| $in^2$ | square inches | 645.2 | square millimeters | $mm^2$ |
| $ft^2$ | square feet | 0.093 | square meters | $m^2$ |
| $yd^2$ | square yard | 0.836 | square meters | $m^2$ |
| ac | acres | 0.405 | hectares | ha |
| $mi^2$ | square miles | 2.59 | square kilometers | $km^2$ |
| | | **VOLUME** | | |
| fl oz | fluid ounces | 29.57 | milliliters | mL |
| gal | gallons | 3.785 | liters | L |
| $ft^3$ | cubic feet | 0.028 | cubic meters | $m^3$ |
| $yd^3$ | cubic yards | 0.765 | cubic meters | $m^3$ |
| | NOTE: volumes greater than 1000 L shall be shown in $m^3$ | | | |
| | | **MASS** | | |
| oz | ounces | 28.35 | grams | g |
| lb | pounds | 0.454 | kilograms | kg |
| T | short tons (2000 lb) | 0.907 | megagrams (or "metric ton") | Mg (or "t") |
| | | **TEMPERATURE (exact degrees)** | | |
| °F | Fahrenheit | 5 (F-32)/9<br>or (F-32)/1.8 | Celsius | °C |
| | | **ILLUMINATION** | | |
| fc | foot-candles | 10.76 | lux | lx |
| fl | foot-Lamberts | 3.426 | $candela/m^2$ | $cd/m^2$ |
| | | **FORCE and PRESSURE or STRESS** | | |
| lbf | poundforce | 4.45 | newtons | N |
| $lbf/in^2$ | poundforce per square inch | 6.89 | kilopascals | kPa |

### APPROXIMATE CONVERSIONS FROM SI UNITS

| Symbol | When You Know | Multiply By | To Find | Symbol |
|---|---|---|---|---|
| | | **LENGTH** | | |
| mm | millimeters | 0.039 | inches | in |
| m | meters | 3.28 | feet | ft |
| m | meters | 1.09 | yards | yd |
| km | kilometers | 0.621 | miles | mi |
| | | **AREA** | | |
| $mm^2$ | square millimeters | 0.0016 | square inches | $in^2$ |
| $m^2$ | square meters | 10.764 | square feet | $ft^2$ |
| $m^2$ | square meters | 1.195 | square yards | $yd^2$ |
| ha | hectares | 2.47 | acres | ac |
| $km^2$ | square kilometers | 0.386 | square miles | $mi^2$ |
| | | **VOLUME** | | |
| mL | milliliters | 0.034 | fluid ounces | fl oz |
| L | liters | 0.264 | gallons | gal |
| $m^3$ | cubic meters | 35.314 | cubic feet | $ft^3$ |
| $m^3$ | cubic meters | 1.307 | cubic yards | $yd^3$ |
| | | **MASS** | | |
| g | grams | 0.035 | ounces | oz |
| kg | kilograms | 2.202 | pounds | lb |
| Mg (or "t") | megagrams (or "metric ton") | 1.103 | short tons (2000 lb) | T |
| | | **TEMPERATURE (exact degrees)** | | |
| °C | Celsius | 1.8C+32 | Fahrenheit | °F |
| | | **ILLUMINATION** | | |
| lx | lux | 0.0929 | foot-candles | fc |
| $cd/m^2$ | $candela/m^2$ | 0.2919 | foot-Lamberts | fl |
| | | **FORCE and PRESSURE or STRESS** | | |
| N | newtons | 0.225 | poundforce | lbf |
| kPa | kilopascals | 0.145 | poundforce per square inch | $lbf/in^2$ |

*SI is the symbol for the International System of Units. Appropriate rounding should be made to comply with Section 4 of ASTM E380.
(Revised March 2003)

# TABLE OF CONTENTS

## LIST OF FIGURES

## LIST OF TABLES



## LIST OF EQUATIONS

## EXECUTIVE SUMMARY

Winter weather conditions often cause serious hazards to travelers on the highway network throughout Wyoming. Snow fence is considered an effective method to reduce low visibility and low friction of the road surface under winter weather conditions. However, it is hard to obtain winter weather data necessary for snow fence design in remote parts of Wyoming. The purpose of this project is to provide seamless wind field and snow precipitation data under adverse winter storm condition using a numerical weather prediction model. The North American Regional Reanalysis (NARR) data were dynamically downscaled using the Weather Research and Forecasting (WRF) model to a 4 km (2.5 mi) resolution over Wyoming in the historical winter storm periods during 1980-2014. The simulated wind fields were checked using the wind records at airport sites in Wyoming in terms of wind statistics. Although the regional mean air temperature has been increasing over the last 34 years, the numbers of windy days (wind speed > 5.4 m/s [12 miles per hour]) were found to be increasing. The WRF-simulated precipitation data were assimilated with the PRISM data, in order to obtain the accurate hourly snow precipitation data. Combining all weather variables, the number of blowing snow events is increasing despite the increasing temperature because of the sufficiently cold winters of Wyoming. Finally, the existing manually observed wind data by Dr. Tabler (Tabler data), which has been used for the snow fence design, were verified by the simulated prevailing wind direction map. It was confirmed that the existing snow fence system is effective under the winter season prevailing wind field since the simulation agreed with the Tabler data. However, it was also found that the simulated wind patterns during the blowing snow events can be quite different from the winter season average prevailing wind map. Moreover, the historical wind statistics indicated that the actual wind had high deviations from the prevailing wind direction, especially along the I-80 corridor.

# CHAPTER 1 INTRODUCTION

## 1.2 Background

The highway system in Wyoming has always suffered from adverse winter weather conditions. To suppress the blowing snow and snow drift, the first stretch of snow fence was installed on I-80 in 1971 (WYDOT, 2009). Since then, the Wyoming Department of Transportation (WYDOT) has developed one of the most extensive snow fence systems in the country.

Extensive research on blowing snow and wind conditions has been conducted by Wyoming for over 40 years. Most notable is the work of Dr. Ronald Tabler, who developed an international reputation as one of the founding fathers of snow blowing and snow fence research (Tabler, 1988; 1991a; 1991b; 1994; 2003). Dr. Tabler's work, hereinafter referred to as Tabler's work, has been incorporated into WYDOT's road design practices, snow fence design, and implementation measures, and has led to reduced crashes and road closures on Wyoming highways (Tabler and Meena, 2006).

Placement and size of snow fence are mainly determined by two important variables: prevailing wind direction and annual snowfall. WYDOT also looks at land availability along highways when considering placement and size. The current snow fence system in Wyoming was installed based on the manually-measured wind direction and the National Climate Data Center (NCDC) annual snowfall records compiled by Dr. Tabler in the early 1990s. In the present report, this existing fundamental weather data shall be herein referred to as "Tabler data".

An example of a snow fence system analysis around the Arlington junction, on I-80, in Wyoming, is shown in Figure 1. The protected green-colored and unprotected red-colored sections are visualized in this figure assuming the wind direction perpendicular to the existing snow fence angles that were placed based on the Tabler data. Note that the efficiency of the snow fence system depends on the actual wind direction rather than the prevailing wind direction. Figure 1 also shows the locations of the Tabler data points (yellow square dots) that depended on the accessibility to the site. The density of the Tabler data points around the Arlington site is relatively high because this section is one of the worst blowing snow areas on I-80 and near the site of Tabler's original research in Wyoming.

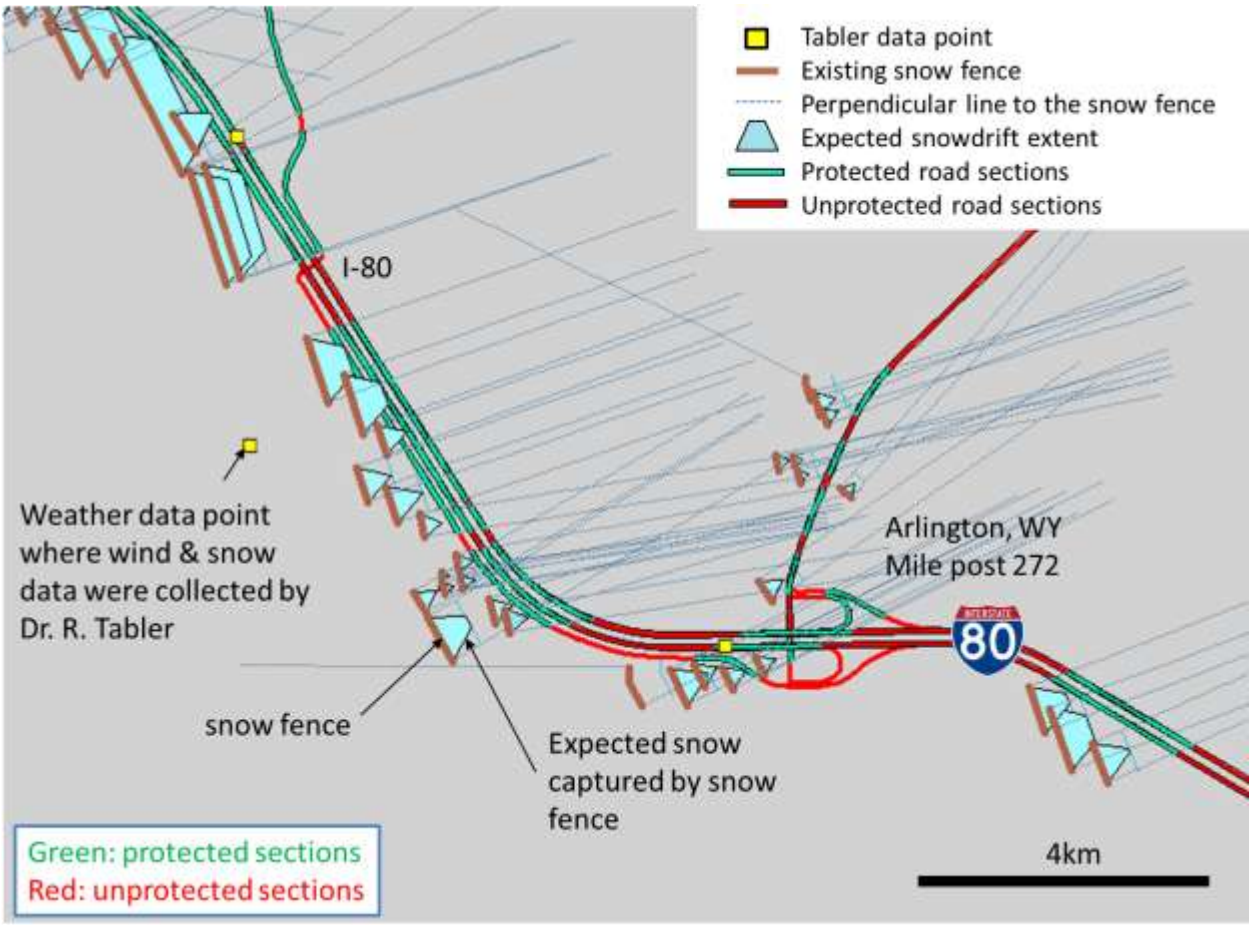


**Figure 1 – Example of snow fence system design around Arlington, WY**

The complete wind direction and annual snowfall in the Tabler data are shown in Figure 2 and Figure 3, respectively. To obtain this information, Dr. Tabler manually collected multiple wind direction data using a handheld anemometer at numerous sites. However, the data collection frequency and timing are not known. The annual snowfall data were developed from the data of the snow course, snow pillow surveys (including the Snow Telemetry (SNOTEL)), and precipitation gauges until the 1990s. The average length of the records is 37.7 years, and the number of the sites is 319. Dr. Tabler's collection of snow survey data tended to take place in high elevation locations while the wind data points were recorded along highways. Thus, the locations and accuracy levels of the wind and the snow data varied. However, the Tabler data are considered the most complete and fine-resolutioned, observation-based weather statistics in Wyoming.

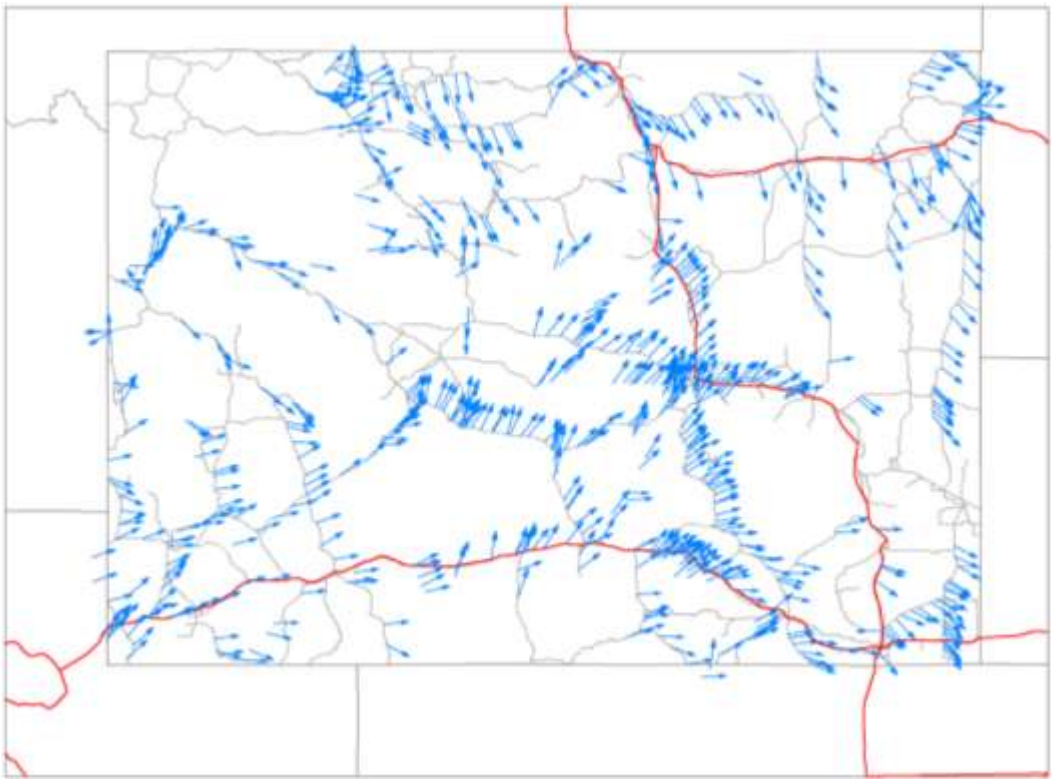

**Figure 2 – Visualized wind direction map using Tabler data**

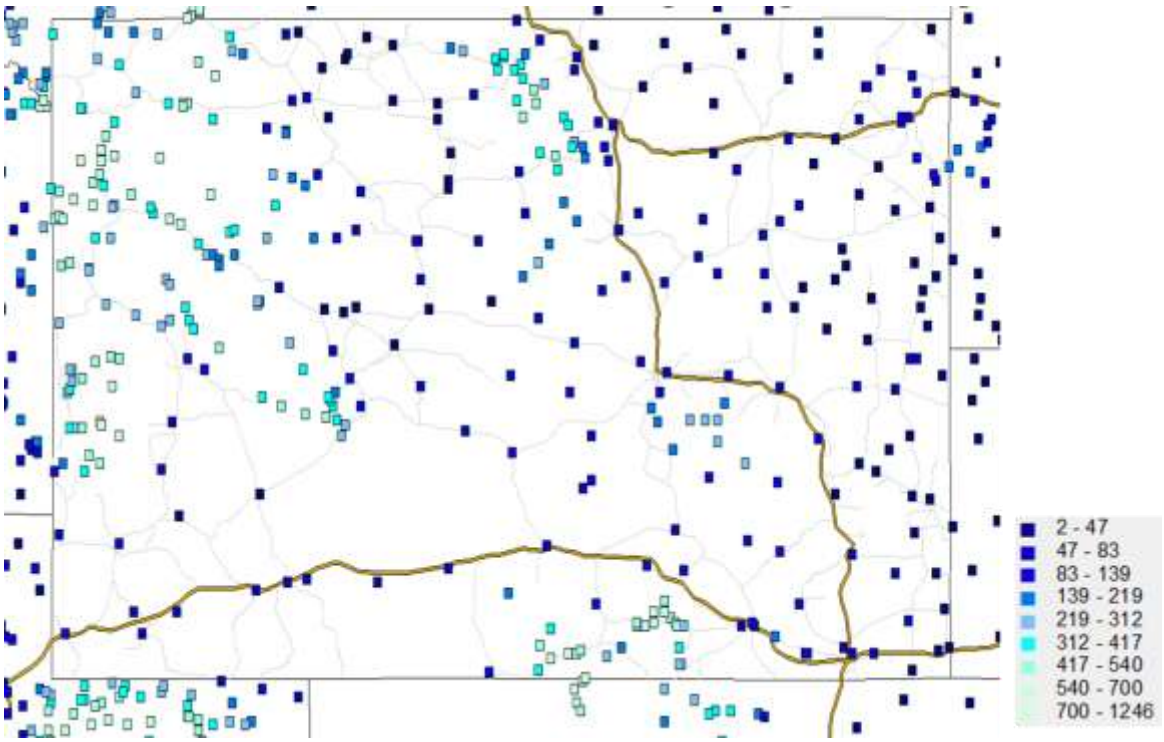


**Figure 3 - Visualized annual snowfall (mm) map using Tabler data**

Although the performance of the snow fence depends on the actual wind direction, it is difficult to record accurate actual wind direction data, especially in remote sections of the Wyoming highway system during the winter weather period. Figure 4 shows the sample wind field simulated by the numerical weather model during an April 2013 winter storm event in southeast Wyoming. This pilot model simulation showed that the wind field was extremely dynamic during the April 2013 winter storm event. This suggested that the wind fields are likely to keep changing and are very heterogeneous during blowing snow events.

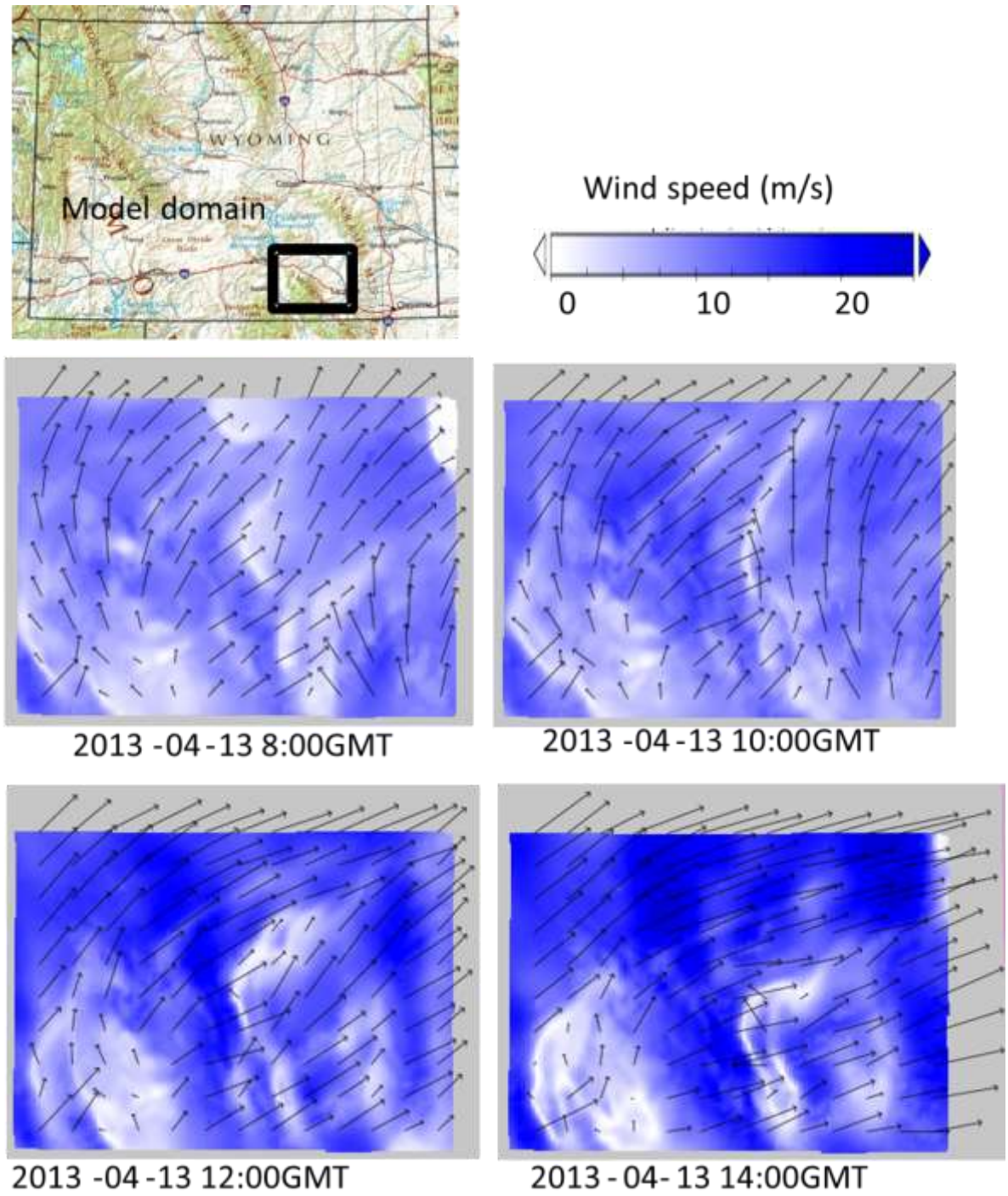


**Figure 4 – Pilot simulation result: wind fields during April-2013 winter storm event along I-80 in Wyoming**

The effect of changing wind direction is considered in the snow fence system by designing overlapping fences and extending fences to incorporate changes in wind direction. However, the true effectiveness of the existing system cannot be evaluated without the complete wind field information. In order to improve and determine the placement and size of snow fences, it is

desirable to estimate the winter wind field using a state-of-the-art numerical weather model, and to assess the historical wind and snow precipitation data used by Winter Research and other programs in WYDOT.

Regional numerical weather models are effective tools for reconstructing the historical weather statistics in a sparsely gauged area such as Wyoming. Numerical weather modeling has become increasingly essential for daily weather forecasting over the past few decades (e.g. Lynch 2008). Such models can also be used for the reconstruction of historical weather conditions by downscaling larger scale reanalysis dataset, such as the North American Regional Reanalysis (NARR, Mesinger et al., 2006). These models are readily available for fine and reliable regional weather information during historical periods when combining the data assimilation with the existing observation data.

Using the Weather Research and Forecasting (WRF) model, which was developed by various US research centers (Leung et al. 2006, Skamarock et al. 2008), this project reconstructed the historical weather conditions that are essential for snow fence design (Tabler 2003). The WRF model is widely used in operational and research applications. The WRF model solves the non-hydrostatic version of the Navier-Stokes equations using a forth order Runge-Kutta scheme using a finite difference method. The outputs of the model provided full atmospheric information, including but not limited to: rain, snow, temperature, atmospheric moisture, pressure, radiation, and wind. The output frequency of the WRF model was hourly or finer, which is sufficient to derive the weather data for the wind field and blowing snow assessment.

The initial and boundary conditions of the WRF model were prepared using the North America Regional Reanalysis (NARR) data (http://www.esrl.noaa.gov/psd/data/gridded/data.narr.html). The NARR project covers the North American Region and the model uses the 32 km resolution National Centers for Environmental Prediction (NCEP) Eta Model together with the Regional Data Assimilation System (RDAS). The NARR dataset includes the atmospheric variables at 3-hour intervals at 29 atmospheric layers. This modeling project provided the seamless and continuous weather conditions during blowing snow events in Wyoming.

## 1.2 Problem Description

Snow fence is an effective mitigation measure for hazardous high wind and blowing snow in Wyoming. The snow fence size and placement are determined by prevailing wind direction and snowfall data. This project evaluates and updates the wind and snow precipitation data by a numerical weather prediction model (WRF). A snow fence system supported by better weather information would inherently improve the safety of the Wyoming transportation system. Therefore, the direct benefits of this research will be a more robust transportation system with fewer traffic crashes, as well as reduced road closures (frequency and duration). This research is directly related to WYDOT's strategic goals including: keeping people safe on the state transportation system, impacts on the environment, new knowledge, and the state of good repair.

## 1.3. Objectives

The main objective of this study is to update wind and winter precipitation information for snow fence design using a numerical weather model during a sufficiently long period so that it can capture the evolving climatic effect. The specific objectives are:

1. To develop new wind and winter precipitation tables for snow fence design using the WRF model.
2. To compare the existing Tabler data to the new data to determine if there have been significant changes in what WYDOT has been using.
3. To determine the appropriate timeframe and frequency for continuous data updating.

# CHAPTER 2 WORK PERFORMED

## Phase 1: Wind condition assessment

During this phase of the project, the WRF model was applied to the State of Wyoming to reconstruct the historical wind conditions. The main outcome was the model-driven wind statistics in an ArcGIS shapefile format in a 4 km (2.5 mi) resolution grid across Wyoming. The simulation was carried out using the WRF model with the boundary conditions estimated from the NARR data. Subtasks for Phase 1 were:

### 1) Initial data analysis using 12 km (7.5 mi) resolution data

The continuous simulation data at a course resolution (12 km (7.5 mi)) from 1980 to 2014 were analyzed. The WRF outputs were validated using wind records at the airport sites. This simulation also identified the winter blowing snow events (wind speed > 5.4 m/s (12mph)) in the historical period.

### 2) WRF model configuration for finer resolution simulation

The model domains for Wyoming were arranged for optimal performance and computational efficiency at a 4 km (2.5 mi) resolution. Then, the test simulations were performed at a workstation to find the best model option for the long-term simulation.

### 3) Model implementation

The configured WRF model was implemented in four workstations at the University of Wyoming for efficiency of the data processing. The very large four-dimensional WRF outputs in Network Common Data Form (NetCDF) format were converted into compact binary format to increase data manageability.

### 4) Wind data processing

The WRF outputs were compared against the Tabler data to check the performance of the model. Then the prevailing wind direction, standard deviation of wind direction, wind speed during the entire simulation period (the winter months), and the winter blowing snow events (wind speed > 5.4 m/s (12mph)) in 1980-2014 were computed. These wind statistics were converted to an ArcGIS shapefile for snow fence design.

## Phase 2: Snow condition assessment

The model-based precipitation and snow condition simulation in the historical period (1981-2014) was performed in this phase. The outcome was the model-driven snow statistics at every 4 km (2.5 mi) resolution node in Wyoming in the ArcGIS shapefile format. Subtasks for Phase 2 were:

### 1) Data assimilation to existing historical records

The WRF output was compared against the existing ground-observed data to evaluate the model errors. The anticipated model biases in the modeled precipitation were corrected using existing historical climatological data such as the PRISM data (the Parameter-elevation Regressions on

Independent Slopes Model, PRISM Climate Group, Oregon State University, http://prism.oregonstate.edu). The model biases were measured as scaling factors between the simulations and the observations in this study. The assimilated (or bias-corrected) WRF simulations are consistent with the monthly precipitation in the PRISM data.

**2) Winter precipitation data compilation for snow fence design**

The bias-corrected model outputs were used for annual mean snowfall and precipitation estimation in Wyoming. The derived quantities were converted into an ArcGIS shapefile for use in snow fence design.

# CHAPTER 3 IMPLEMENTATION AND RESULTS

## Phase 1: Wind condition assessment

### 1) Initial data analysis using 12 km (7.5 mi) resolution data

The continuous WRF simulation at 12 km (7.5 mi) resolution was performed previously for other hydrological research. The model parameter selections are identical to the 4 km (2.5 mi) configuration described in the following sections, except for domain sizing. The detailed documentation is available in Heward (2015) and Johnson (2015). The continuous WRF simulation data were used for winter precipitation analyses as well as the blowing snow condition identification in the historical period of October 1980 through September 2014 (water years 1981-2014). Note that a water year starts on October 1 in the year before and ends on September 30 of the following year.

The simulation results were stored in a binary format file. A program (Windstat5, ©2015-17 Noriaki Ohara) has been developed to convert the binary WRF output to a common surface data format. The specification of the format is available at http://www.webmet.com/MetGuide/Samson.html. This format is supported in the wind visualization software, WRPLOT View™ (© 1995-2017 Lakes Environmental Software). More information about this free Windows application is available at http://www.webmet.com/software.html#WRPLOT. The developed software is able to extract the simulated wind at any location in Wyoming. The wind field was visualized using a frequency distribution histogram and a wind rose, which is a wind direction and speed diagram. Figure 5 shows an example of wind roses at eight selected locations in Wyoming, during the year 1992, and illustrates the variety of wind statistics in Wyoming. It is now possible to extract wind statistics during 1980-2014 at any location in Wyoming using the developed software.

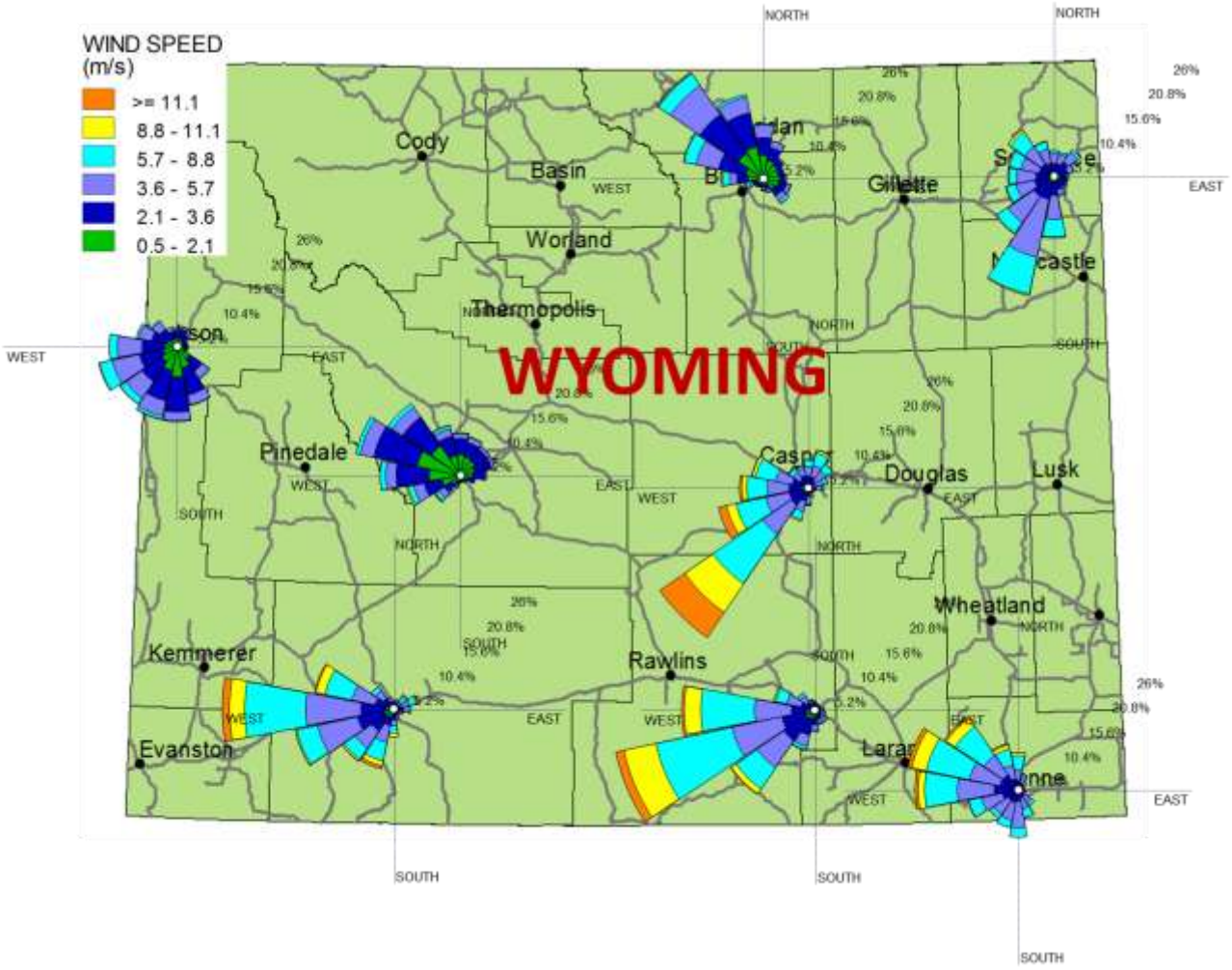


**Figure 5- Wind roses based on the WRF simulation at eight selected locations in 1992**

***Validation of the simulated wind field***

The modeled wind field was validated by the observed wind records at five airport sites from Support Center for Regulatory Atmospheric Modeling (SCRAM) Surface Meteorological Archived Data (1984-1992). The airports from the SCRAM database that were used are:

1. WY24018 Cheyenne/Cheyenne Regional Airport.
2. WY24021 Lander/Hunt Field.
3. WY24027 Rock Springs/Sweetwater County Airport.
4. WY24029 Sheridan/Sheridan County Airport.
5. WY24089 Casper/Natrona County International Airport.

The geographic locations of the airports are shown in Figure 6.

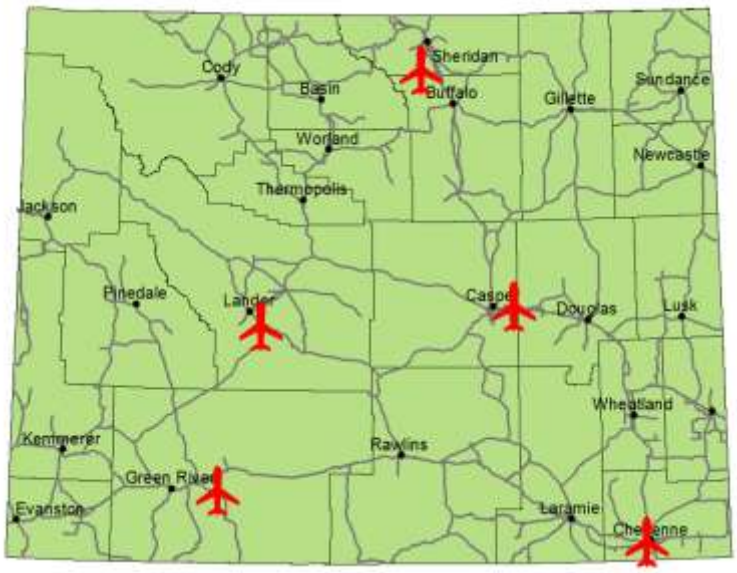


**Figure 6 - The locations of the airports in Wyoming in the SCRAM database**

Example comparisons at these five airports are outlined in Figure 7 through Figure 11. Considering the high variability of the wind, the comparisons of simulated and observed wind statistics showed good agreement at these five locations. This model simulation is realistic for engineering practices. The numerical model-based wind fields are highly valuable in the areas between these observation sites.

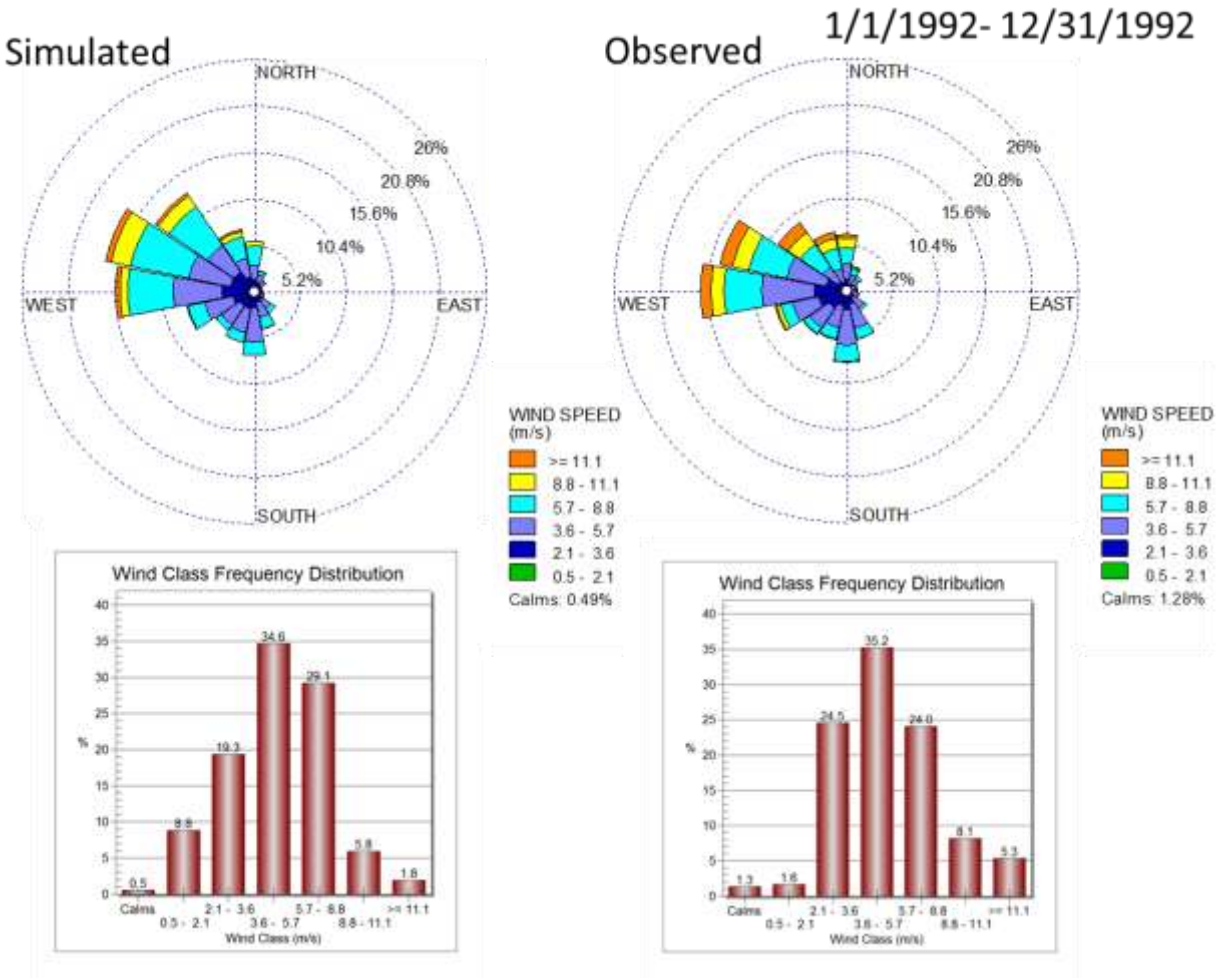


**Figure 7- Model validation using observed wind record during 1992 at the Cheyenne Regional Airport**

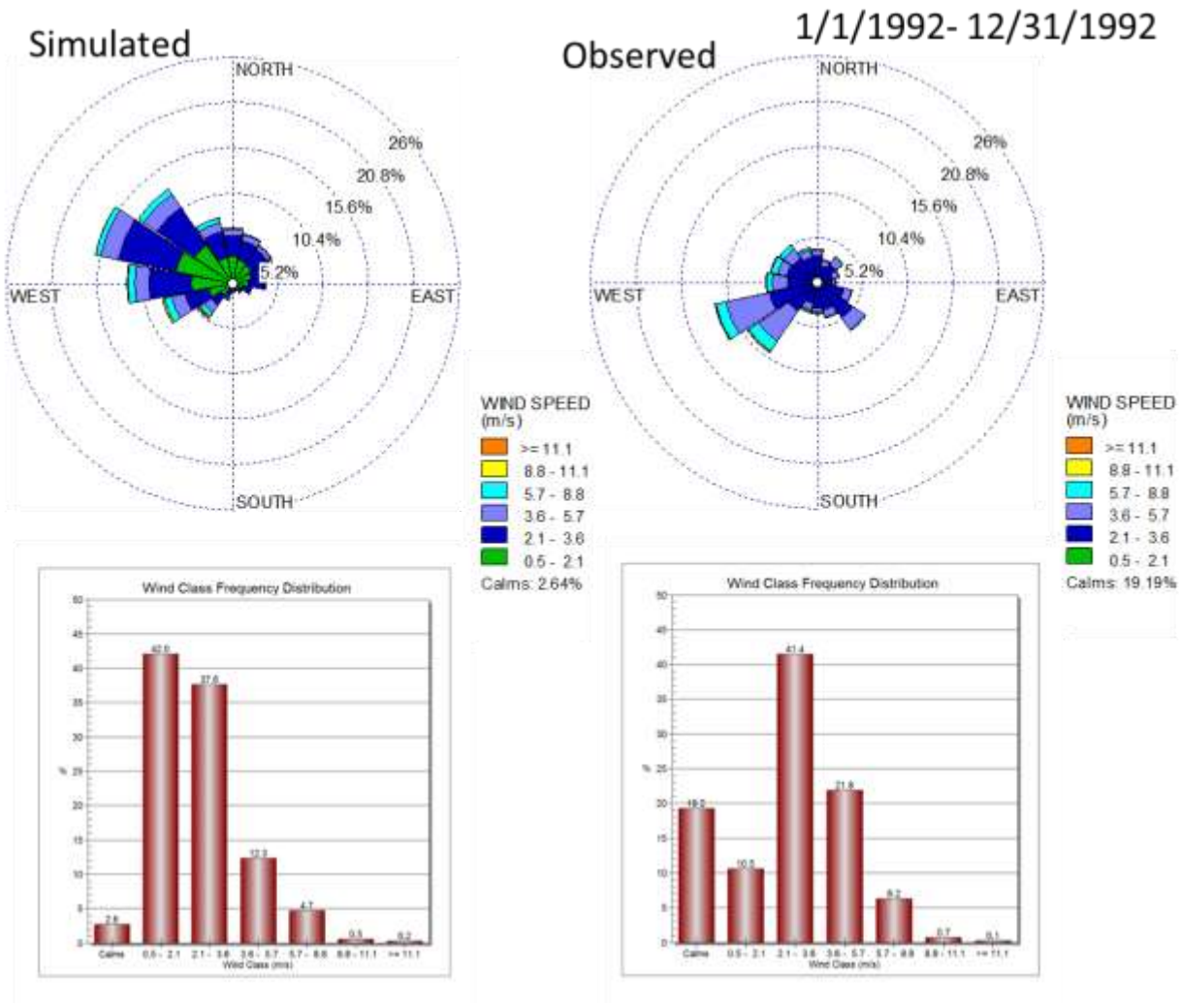


**Figure 8 -Model validation using observed wind record during 1992 at Hunt Field**

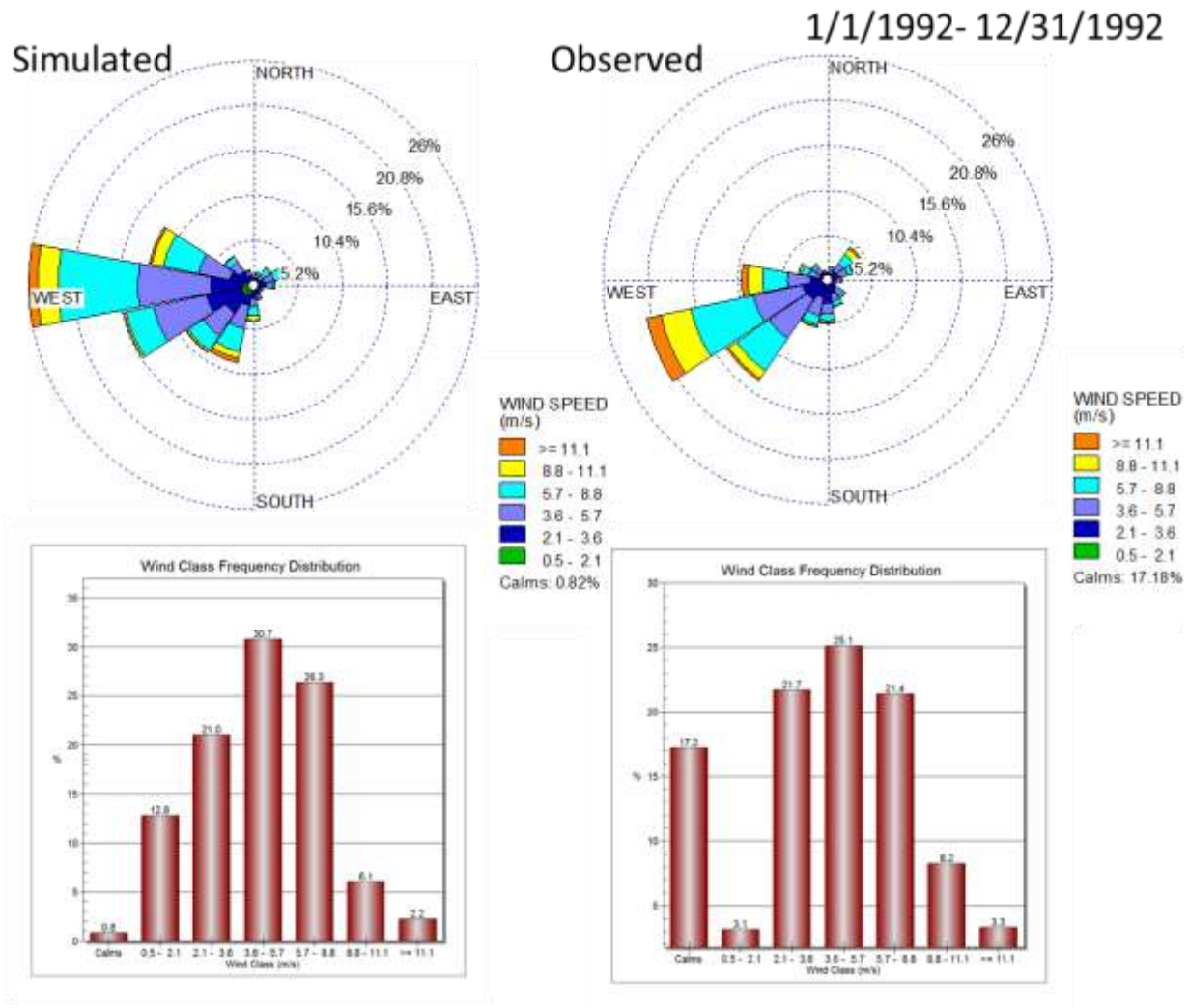


**Figure 9 - Model validation using observed wind record during 1992 at the Sweetwater County Airport**

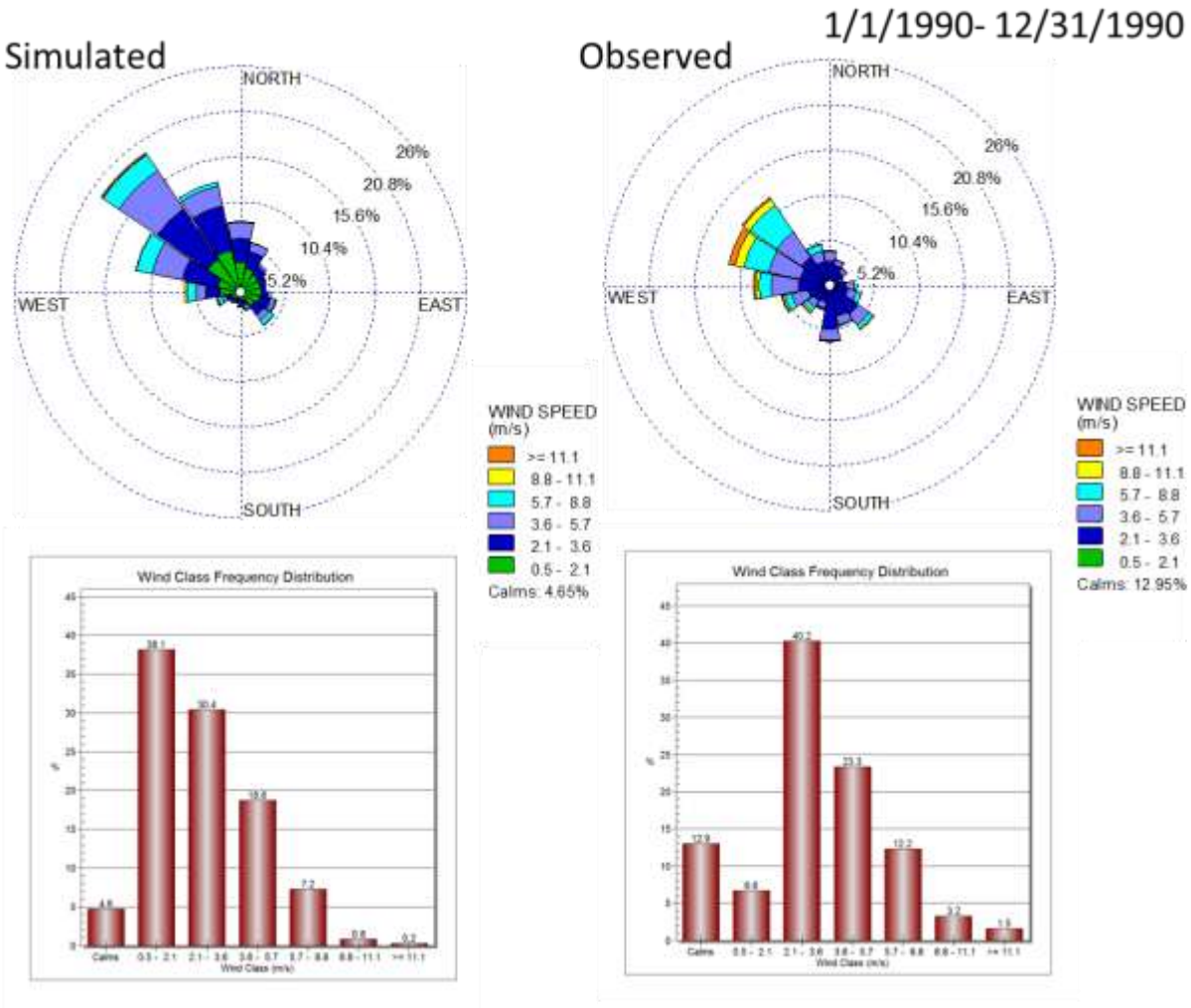


**Figure 10 - Model validation using observed wind record during 1990 at the Sheridan County Airport. (Note: The data in 1992 was missing in the SCRAM database while the WRF data has complete spatial and temporal coverages.)**

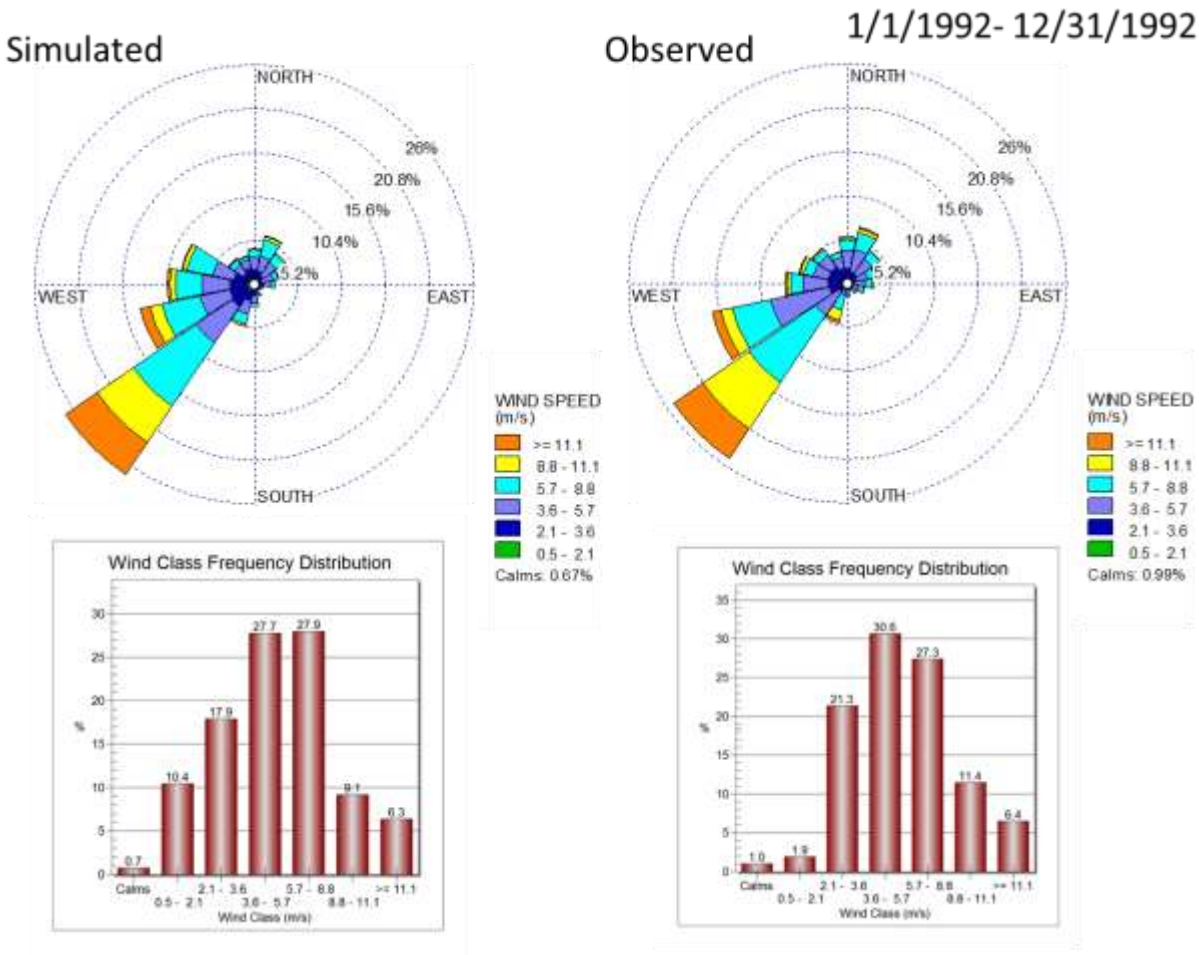


**Figure 11 - Model validation using observed wind record during 1992 at the Natrona County International Airport**

***Wind field trend analysis***

This section presents the wind field trend analysis using the modeled long-term wind data in Wyoming. First, threshold wind speed for the "windy" period was defined. The most common wind classification developed by Beaufort (Saucier, 2003) is shown in Table 1. Note: The wind speed in this report is at 10 meter (32.8 feet) above the ground based on the Beaufort's table. In this study, the threshold was set at 5.4 m/s (12 mph or 19.3 km/h) as fresh powdery snow typically starts moving at this wind speed.

**Table 1 - Wind classification based on Beaufort wind force scale**

| Force | Speed | | | Name | Conditions at Sea | Conditions on Land |
|---|---|---|---|---|---|---|
| | knots | km/h | mi/h | | | |
| 0 | < 1 | < 2 | < 1 | Calm | Sea like a mirror. | Smoke rises vertically. |
| 1 | 1-3 | 1-5 | 1-4 | Light air | Ripples only. | Smoke drifts and leaves rustle. |
| 2 | 4-6 | 6-11 | 5-7 | Light breeze | Small wavelets (0.2 m). Crests have a glassy appearance. | Wind felt on face. |
| 3 | 7-10 | 12-19 | 8-11 | Gentle breeze | Large wavelets (0.6 m), crests begin to break. | Flags extended, leaves move. |
| 4 | 11-16 | 20-29 | 12-18 | Moderate breeze | Small waves (1 m), some whitecaps. | Dust and small branches move. |
| 5 | 17-21 | 30-39 | 19-24 | Fresh breeze | Moderate waves (1.8 m), many whitecaps. | Small trees begin to sway. |
| 6 | 22-27 | 40-50 | 25-31 | Strong breeze | Large waves (3 m), probably some spray. | Large branches move, wires whistle, umbrellas are difficult to control. |
| 7 | 28-33 | 51-61 | 32-38 | Near gale | Mounting sea (4 m) with foam blown in streaks downwind. | Whole trees in motion, inconvenience in walking. |
| 8 | 34-40 | 62-74 | 39-46 | Gale | Moderately high waves (5.5 m), crests break into spindrift. | Difficult to walk against wind. Twigs and small branches blown off trees. |
| 9 | 41-47 | 76-87 | 47-54 | Strong gale | High waves (7 m), dense foam, visibility affected. | Minor structural damage may occur (shingles blown off roofs). |
| 10 | 48-55 | 88-102 | 55-63 | Storm | Very high waves (9 m), heavy sea roll, visibility impaired. Surface generally white. | Trees uprooted, structural damage likely. |
| 11 | 56-63 | 103-118 | 64-73 | Violent storm | Exceptionally high waves (11 m), visibility poor. | Widespread damage to structures. |
| 12 | 64+ | 119+ | 74+ | Hurricane | 14 m waves, air filled with foam and spray, visibility bad. | Severe structural damage to buildings, wide spread devastation. |

The Wyoming average wind speed was computed for the 34-year period (water years 1981-2014). The computed time series of average wind speed in Wyoming is shown in Figure 12. The yellow and black thick lines in Figure 12 denote the 24-hour moving average and the linear regression line of the time series, respectively. As can be seen, the wind speed has a somewhat clear seasonality, which is higher during winter seasons. Although it is not very clear from the graph, there is an upper trend in the Wyoming average wind speed.

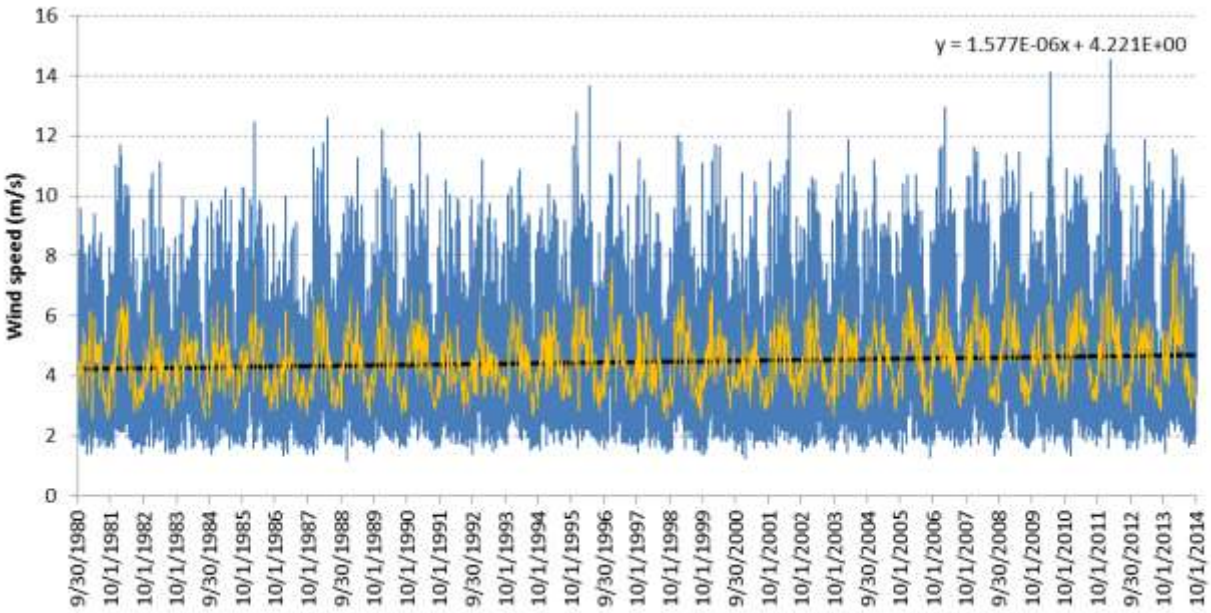


**Figure 12 –Computed Wyoming average wind speed**

Second, the number of days that wind speed exceeds 5.4 m/s (12 mph) was computed for every five-year period from 1980 through 2014, as shown in Figure 13. The analysis revealed that in recent years Wyoming has roughly 20-30 more windy days than in the 1980s. The time series of the computed Wyoming average wind speed showed a slight upward trend in the average wind speed with a rate of 0.138 m/s per decade (0.31 mph per decade).

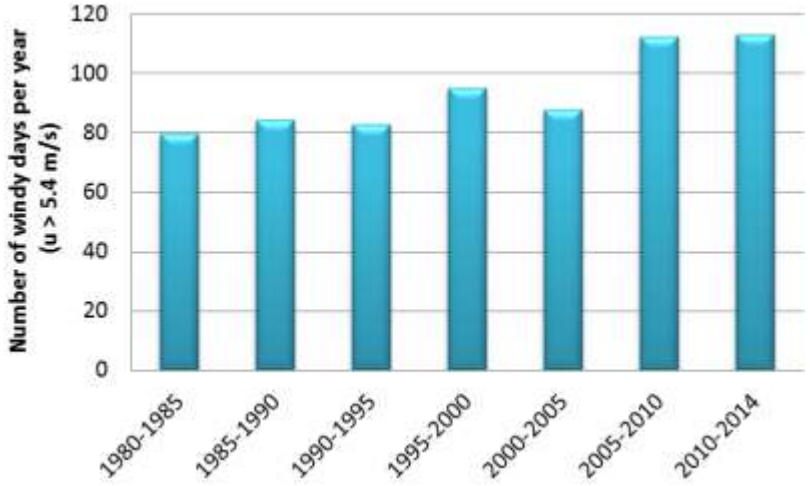


**Figure 13 - Frequency of windy days (wind speed > 5.4 m/s (12 mph)) during the last three+ decades based on the reconstructed Wyoming average wind speed for 1980 – present**

The same analysis was repeated for a point location at Arlington, WY, where frequent blowing snow occurs. Figure 14 shows the number of the windy days at Arlington increased in the long-term simulation.

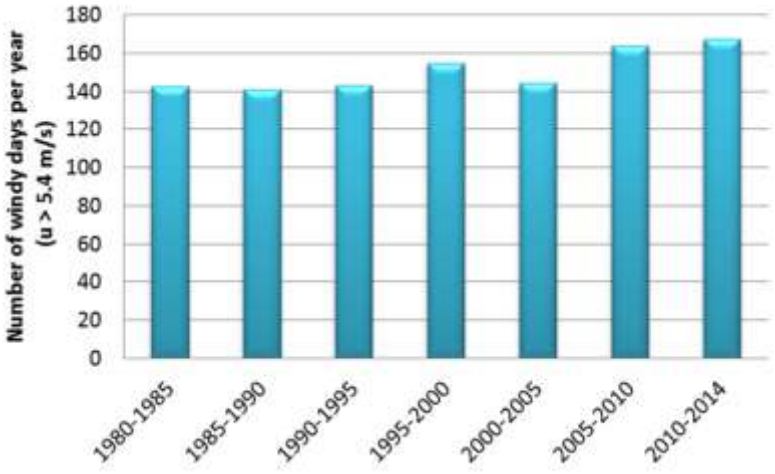


**Figure 14 - Frequency of windy days (wind speed > 5.4 m/s (12 mph)) during the last three+ decades based on the reconstructed average wind speed at Arlington, WY, for 1980 – present**

According to the WRF simulation based on the NARR data, Wyoming has gotten windier over the last three decades. It may be inferred that the increase of wind speeds and number of windy days is likely due to the climate change. However, no consensus in surface wind trend analyses was established due to inconsistency among the historical wind datasets (Intergovernmental Panel on Climate Change (IPCC) Fifth Assessment Report (AR5), Hartmann et al., 2013), although some increase trend in upper-air wind was found over North America in 1979-2005 (Vautard et al., 2010). Coupled Model Intercomparison Project Phase 5 (CMIP5) multi-model projections suggested a systematic increasing trend in upper-air winds in mid-latitude regions toward the end of 21$^{st}$ century. Temperature is a typical index of the energy level and part of the energy may be transformed into kinetic energy, which is observed as wind speed. This explanation is generally acceptable hypothesis while the increasing trends in wind speed are very heterogeneous (Curtis and Grimes, 2004).

### 2) WRF model configuration for finer resolution simulation

The WRF model, configured with double nesting domains is shown in Figure 15. The outer domain (Domain 1) has a 12 km (7.5 mi) resolution, and the inner domain (Domain 2) has 4 km (2.5 mi) resolution. The initial and boundary conditions of the WRF model were prepared from the NARR data (http://www.esrl.noaa.gov/psd/data/gridded/data.narr.html). NARR is the atmospheric reanalysis dataset for the North American Region at a 32 km (20 mi) resolution using both the NCEP Eta Model and the RDAS. The NARR dataset provides 3-hour data at 29

levels and atmospheric state variables that were sufficient for the initial and boundary condition preparation of the WRF model.

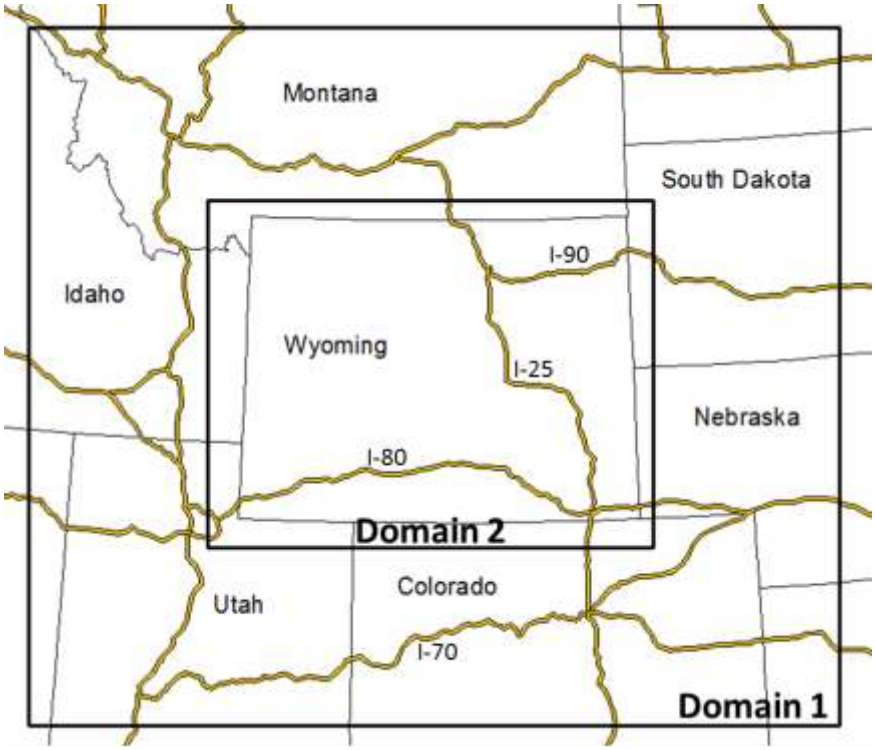


**Figure 15 - The nesting domains of the WRF model for wind field reconstruction**

There are several parameterization options in the WRF model system. Morrison Double Moment scheme (Morrison et al., 2008), Noah Land Surface model (Kusaka et al., 2001), and Yonsei University scheme (Hong et al., 2006) were selected for the cloud microphysics, land surface modeling, and the planetary boundary layer (PBL) options, respectively. These model configurations were primarily optimized for the precipitation on the ground in Wyoming (Heward, 2015).

Data processing, adjustment, and transfer using the supercomputers at the Advanced Research Computing Center (ARCC), at the University of Wyoming, were found to be extremely time consuming. To accelerate the computation, three workstations were integrated into the computational system in the researcher's office at the University of Wyoming. A cost-performance efficiency comparison was carried out between a new high-end desktop (Intel Core i7-5820K Haswell-E 6-Core 3.3 GHz Processor) and the three, second-hand, industry-class workstations (Intel Xeon E3-1245 3.3GHz Processor). Based on the CPU benchmark (https://www.cpubenchmark.net/), it was concluded that the three used workstations were about two times faster than the single new computer for the same cost. As such, three used workstations were purchased for this project. The conventional operating system, Linux Mint (Rose), and other necessary software such as WRF, NetCDF, vim, ssh server, NFS server, and

GNU compilers, were installed. The routine computation scheduling scheme using a script language (bash) was established at the University of Wyoming to implement the model computation efficiently.

**3) Model implementation**

Since the high-resolution WRF simulation was found to be more time-consuming than the original estimation, the focus became on simulating the blowing snow periods rather than the entire historical period.

The continuous simulation at a course resolution (12 km (7.5 mi)) from 1980 to 2014 was used to identify the winter blowing snow events (wind speed > 5.4 m/s (12 mph)) during the historical period. Then the computationally more expensive fine resolution (4 km (2.5 mi)) simulation was implemented for detailed analyses during the identified blowing snow event periods. Thus, the blowing snow periods were identified based on the outputs of the numerical weather model simulation results for the period of 1980-2014 at 12 km (7.5 mi) spatial resolution over Wyoming.

***Modeling of mobile and blowing snow***

It was necessary to characterize the occurrence of blowing snow from the weather variables. Obviously, blowing snow requires strong wind as well as mobile snow, which is loose snow not bonded to a larger mass or ground surface. Hence, the mobile snow amount must be quantified from the atmospheric data to estimate the blowing snow period. However, a practical modeling of the mobile snow is currently lacking. In this project, a simple exponential decay model was proposed for this purpose. Assuming the mobile snow amount exponentially decays in general, it can be modeled as,

$$\zeta(t) = \zeta(t-1) \cdot 0.5^{\,1/t_{half}} \tag{1}$$

$t_{half}$ = half life of the mobile snow [hour]

$\zeta(t)$ = mobile snow at time, t [mm]

This empirical model includes only one parameter, half-life of the mobile snow. The mobile snow stabilizes or sublimates as a function of time since the original snow. Figure 16 shows an example of mobile snow amount estimation using this proposed model with 1 mm [0.039 inch] of snow precipitation. The half-life was set at six hours. This corresponds to the condition that nearly 94 percent of the mobile snow was stabilized or sublimated within 24 hours since the snowfall.

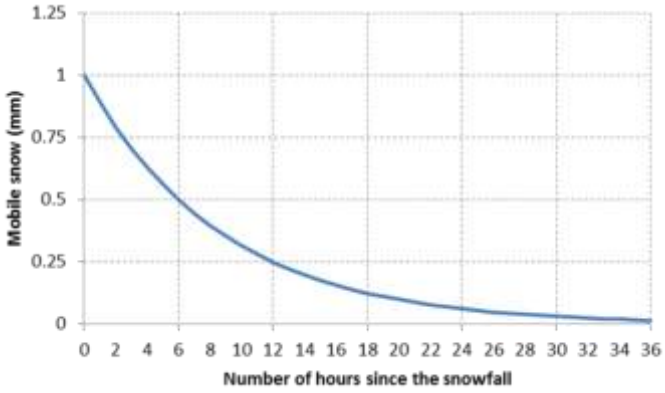


**Figure 16- Proposed one parameter model for mobile snow amount**

An example of a reconstructed blowing snow event using the WRF model around Arlington, WY, is shown in Figure 17. To estimate the blowing snow amount, the following three steps were taken at every single computational node and time step:

1. Separating snowfall and rainfall by air temperature.
2. Computing the mobile snow amount (depth, mm) from the snowfall.
3. Computing the blowing snow amount (depth, mm) from the wind speed.

In step 1, the phase of precipitation was determined from the computed air temperature. The computation of step 2 was described by Equation 1. The blowing snow amount at step 3 was approximated by the mobile snow amount only when wind speed exceeded the threshold (5.4 m/s (12 mph)). That is,

$$Bsnow = \begin{cases} 0, & wind\ speed < 5.4\ m/s \\ \zeta, & wind\ speed \geq 5.4\ m/s \end{cases} \quad (2)$$

where

*Bsnow* = blowing snow depth or amount (mm)

$\zeta$ = mobile snow amount (mm)

This modeling tool can provide an index of the blowing snow amount with the minimum number of the parameters. In this project, the blowing snow depth is just an indicator of blowing snow risk or identification of the blowing snow period under the given weather condition. Therefore, blowing snow modeling will not be discussed further in this report. However, blowing snow

modeling may be identified as a major knowledge gap in this project, and a great future research topic to improve understanding and risk assessment skill of the blowing snow events.

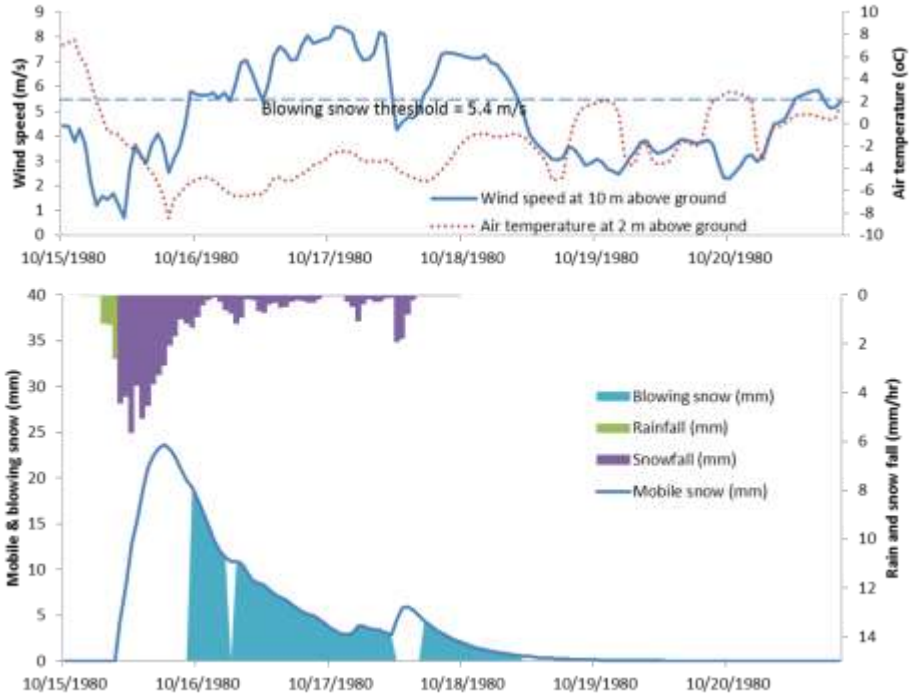


**Figure 17 – Blowing snow amount estimation based on the modeled atmospheric conditions by the WRF model**

Based on the simple exponential blowing snow model, with $t_{half}$ = 6 hours, the blowing snow weeks were identified for the computationally intensive 4 km (2.5 mi) WRF simulations. As visually described in Figure 17, the blowing snow period was defined as the period with more than 1 mm (0.039 in) of blowing snow found at any of the computational cells in the model domain. A partial list of the simulation periods are shown in Table 2. These 500 winter-condition weeks (about 15 weeks per year) of the simulation cover most of the blowing snow periods in the period 1981-2014. Note that the parameter $t_{half}$ should not be sensitive to the blowing snow identification, while the cutoff point of minor blowing snow events may be affected by the choice of the parameter. Finally, the 4 km (2.5 mi) WRF simulation was performed for these 500 winter weather weeks identified by the 12 km (7.5 mi) WRF simulation results for the period of 1981-2014 in Wyoming.

**Table 2 - Partial list of the winter weather periods in 1981-2014**

| rank | **weekname** | Simulation start date | Simulation end date | Number of winter storm hours |
|---|---|---|---|---|
| 1 | **19980111** | 19980110 | 19980118 | 90 |
| 2 | **19961222** | 19961221 | 19961229 | 89 |
| 3 | **19860216** | 19860215 | 19860223 | 79 |
| 4 | **20090329** | 20090328 | 20090405 | 79 |
| 5 | **20051127** | 20051126 | 20051204 | 74 |
| 6 | **19951231** | 19951230 | 19960107 | 56 |
| 7 | **19840422** | 19840421 | 19840429 | 55 |
| 8 | **20090322** | 20090321 | 20090329 | 55 |
| 9 | **20140223** | 20140222 | 20140302 | 54 |
| 10 | **20000109** | 20000108 | 20000116 | 53 |
| 11 | **20081221** | 20081220 | 20081228 | 53 |
| 12 | **19960128** | 19960127 | 19960204 | 52 |
| 13 | **20131201** | 20131130 | 20131208 | 52 |
| 14 | **19811220** | 19811219 | 19811227 | 51 |
| 15 | **19990207** | 19990206 | 19990214 | 51 |
| 16 | **19841125** | 19841124 | 19841202 | 50 |
| 17 | **20030316** | 20030315 | 20030323 | 50 |
| 18 | **20120219** | 20120218 | 20120226 | 49 |
| 19 | **20101121** | 20101120 | 20101128 | 48 |
| 20 | **19860209** | 19860208 | 19860216 | 47 |
| 490 | **19961103** | 19961102 | 19961110 | 1 |
| 491 | **19980412** | 19980411 | 19980419 | 1 |
| 492 | **19981129** | 19981128 | 19981206 | 1 |
| 493 | **20000409** | 20000408 | 20000416 | 1 |
| 494 | **20010218** | 20010217 | 20010225 | 1 |
| 495 | **20020929** | 20020928 | 20021006 | 1 |
| 496 | **20030406** | 20030405 | 20030413 | 1 |
| 497 | **20041031** | 20041030 | 20041107 | 1 |
| 498 | **20090125** | 20090124 | 20090201 | 1 |
| 499 | **20090426** | 20090425 | 20090503 | 1 |
| 500 | **20131013** | 20131012 | 20131020 | 1 |

### 4) Wind data processing

The wind azimuth can be computed from x and y components of wind speed by an arctangent function. The two-argument arctangent function, atan2(y, x) is commonly available to obtain the arctangent of y/x in the range $-\pi$ to $\pi$ radians ( -180 to 180 degrees). However, the zero azimuth in geographic wind is the north (y-axis) instead of the east (x-axis). Also, the azimuth in geographic wind corresponds to the direction the wind comes from. Therefore, the geographical wind direction and wind speed can be computed from westerly and southerly wind components, *u* and *v*, produced in the WRF simulation as,

$$\theta = \text{atan2}(-u, -v) \quad (3)$$

$$Spd = \sqrt{u^2 + v^2} \quad (4)$$

where

$\theta$ = wind azimuth (rad)
$u$ = East-west component of wind speed (m/s, east positive)
$v$ = North-south component of wind speed (m/s, north positive)
$Spd$ = wind speed (m/s)

Note that radians are converted to degrees by multiplying by 180 / π = 57.29578. The reverse conversion can be performed by,

$$u = -Spd\ \sin(\theta) \quad (5)$$

$$v = -Spd\ \cos(\theta) \quad (6)$$

***Yamartino method***

The Yamartino method (Yamartino, 1984) is an algorithm for calculating an approximation to the standard deviation $\sigma_\theta$ of wind direction θ during a single pass through the incoming data. The average values of sin θ and cos θ are first computed.

$$s_a = \frac{1}{n}\sum_{i=1}^{n} \sin\theta_i \quad (7)$$

$$c_a = \frac{1}{n}\sum_{i=1}^{n} \cos\theta_i \quad (8)$$

where i denotes time step, and n is sample size or the number of the total time steps. Then, the average azimuth angle and the standard deviation of the angle can be computed as follows:

$$\theta_a = \text{atan2}(s_a, c_a) \quad (9)$$

$$\sigma_\theta = \arcsin(\varepsilon)\left[1 + \left(\frac{2}{\sqrt{3}} - 1\right)\varepsilon^3\right] \quad (10)$$

where,

$$\varepsilon = \sqrt{1 - (s_a^2 + c_a^2)} \quad (11)$$

***Wind data cross-comparison***

The wind statistics were computed for three different periods: all seasons period, winter season period, and winter storm period.

1. All seasons period: all period including summer seasons
2. Winter season period: October 30-May 1
3. Winter storm period: blowing snow period (more than 1 mm (0.039 in) of blowing snow)

The all seasons period is the entire simulation period between September 30, 1980 and October 1, 2014, including summer seasons. The winter season period consists of the six month periods (October 30-May 1), in each of the following years, 1980-2014. The winter storm period is the period with more than 1 mm [0.039 inch] of blowing snow on the computational cell in 1980-2014. Therefore, the length of the winter storm period depends on geographical location and climate. The statistics for the winter storm period were directly computed from the 4 km (2.5 mi) WRF simulation outputs. However, the other two sets of statistics were calculated from the 12 km (7.5 mi) WRF simulation because the 4 km (2.5 mi) WRF model was applied only during the blowing snow periods. Resampling or spatial interpolation was performed by the inverse-distance 4-point weighting averaging method.

The observed wind direction map in Figure 2, the 1990s Tabler data, was compared to the average of the all seasons period (Figure 18 and Figure 19), the average of the winter season period (Figure 20 and Figure 21), and the average of the winter storm period (Figure 22 and Figure 23). Arrows were placed at the observed wind data points in the Tabler data. The wind directions were computed by inverse distance weighting averaging of four nearest computational nodes. The temporal average wind direction was computed from the methodology presented in the previous section.

The observed wind direction map (the Tabler data) is closest to the winter season mean wind direction. Figure 19, 21, and 23 also show the wind direction correlations between the observation and the simulations. The correlation coefficient (Pearson product-moment correlation coefficient) between the wind azimuth angles of the winter season average and the Tabler data is calculated as 0.49, which indicates the strongest correlation among the three periods. Considering the large spatial and temporal variation of the values, this analysis shows that Tabler's wind table well represented the winter season prevailing wind field. The WRF-simulated wind fields are also realistic in the area between the validation data points at the five airports used for model validation.

Figure 22 demonstrates that the average wind direction map during the winter storm period is quite different from the other maps: all seasons and winter season mean wind direction maps. This figure shows only the average wind directions during the blowing snow events identified in the winter storm period 1980-2014 by the 4 km (2.5 mi) WRF model. The winter storm wind

field, which may be useful to understand the mechanism of road closures and crashes, is typically difficult to obtain through field observations.

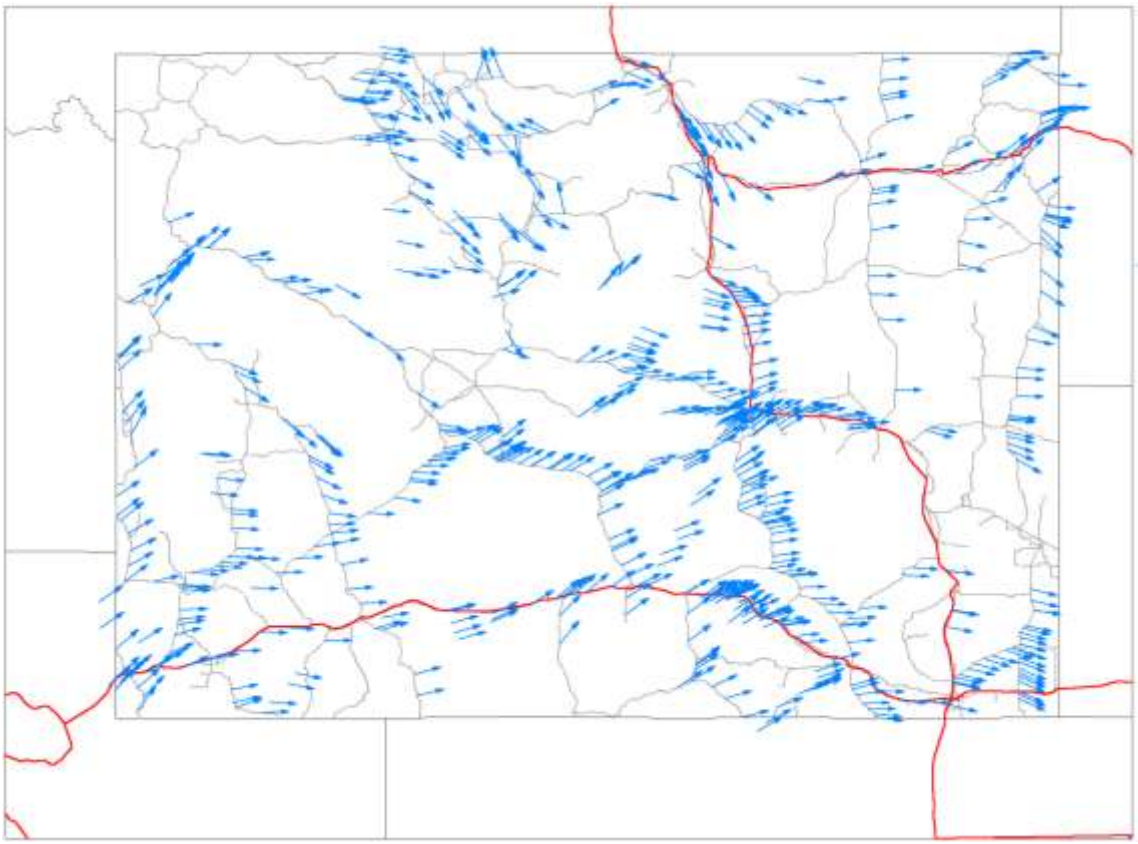

**Figure 18 - Wind direction map of the all seasons period average 1980-2014**

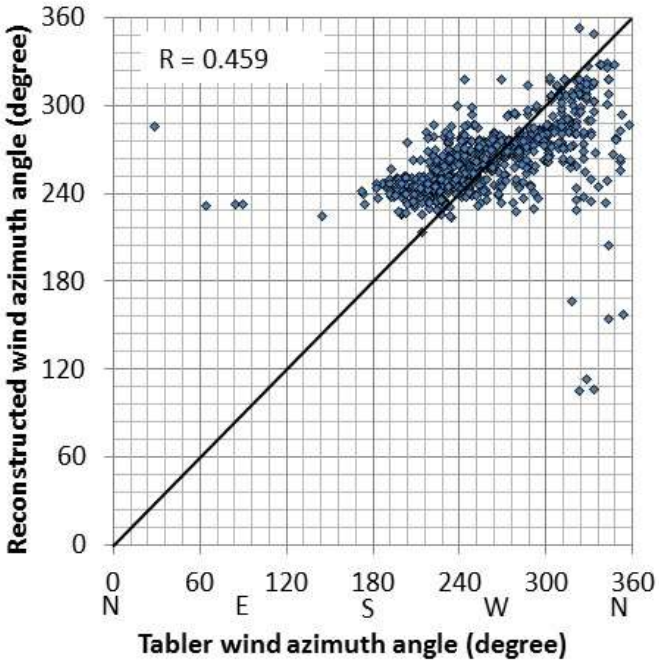


**Figure 19 - Correlation between the simulated and the observed wind azimuth angles at the data points of the Tabler data for all seasons period average 1980-2014**

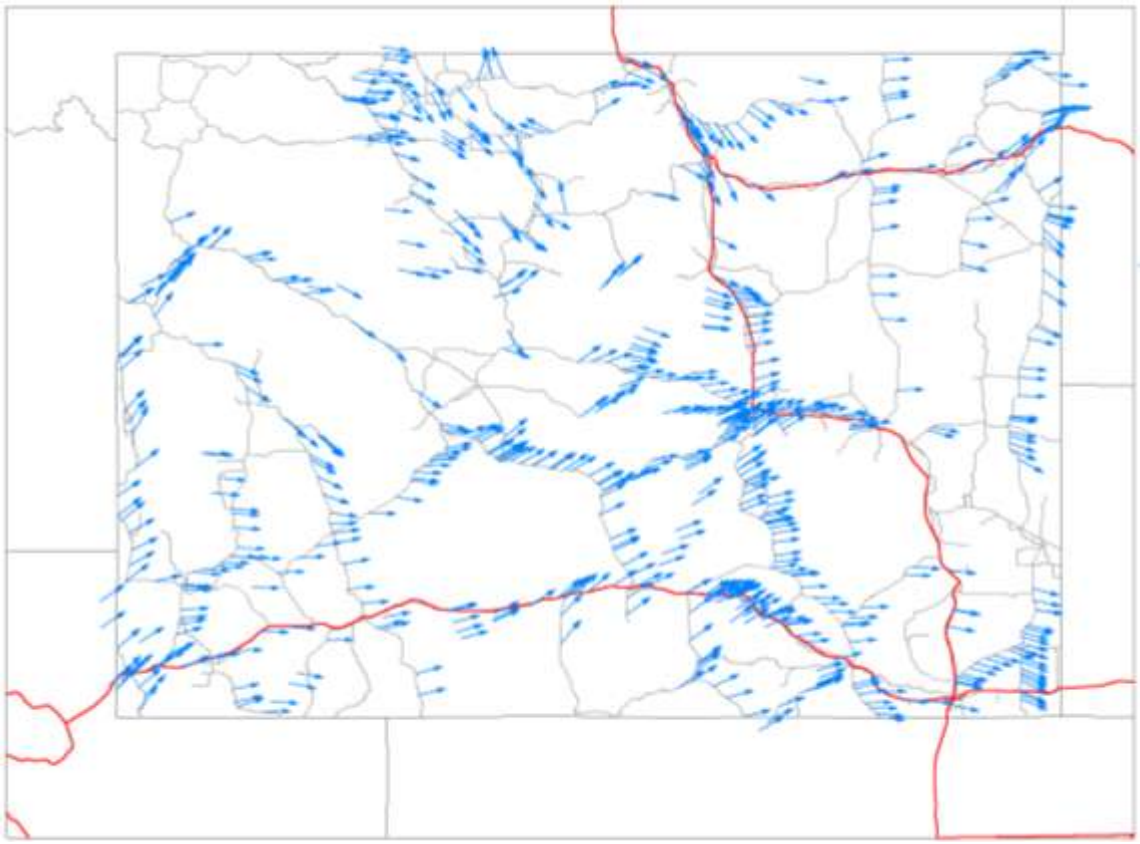

**Figure 20 - Wind direction map of the winter season period average, Oct 30th - May 1st, 1980-2014**

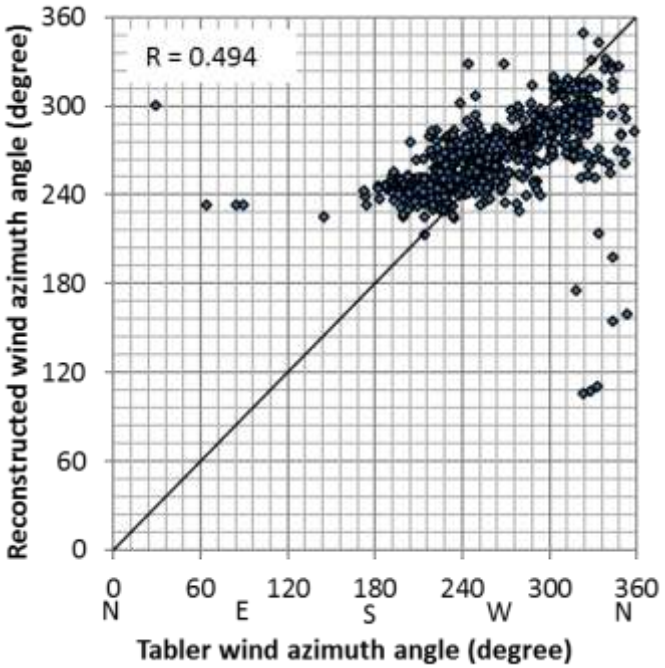


**Figure 21 -Correlation between the simulated and the observed wind azimuth angles at the data points of the Tabler data for winter season period average 1980-2014**

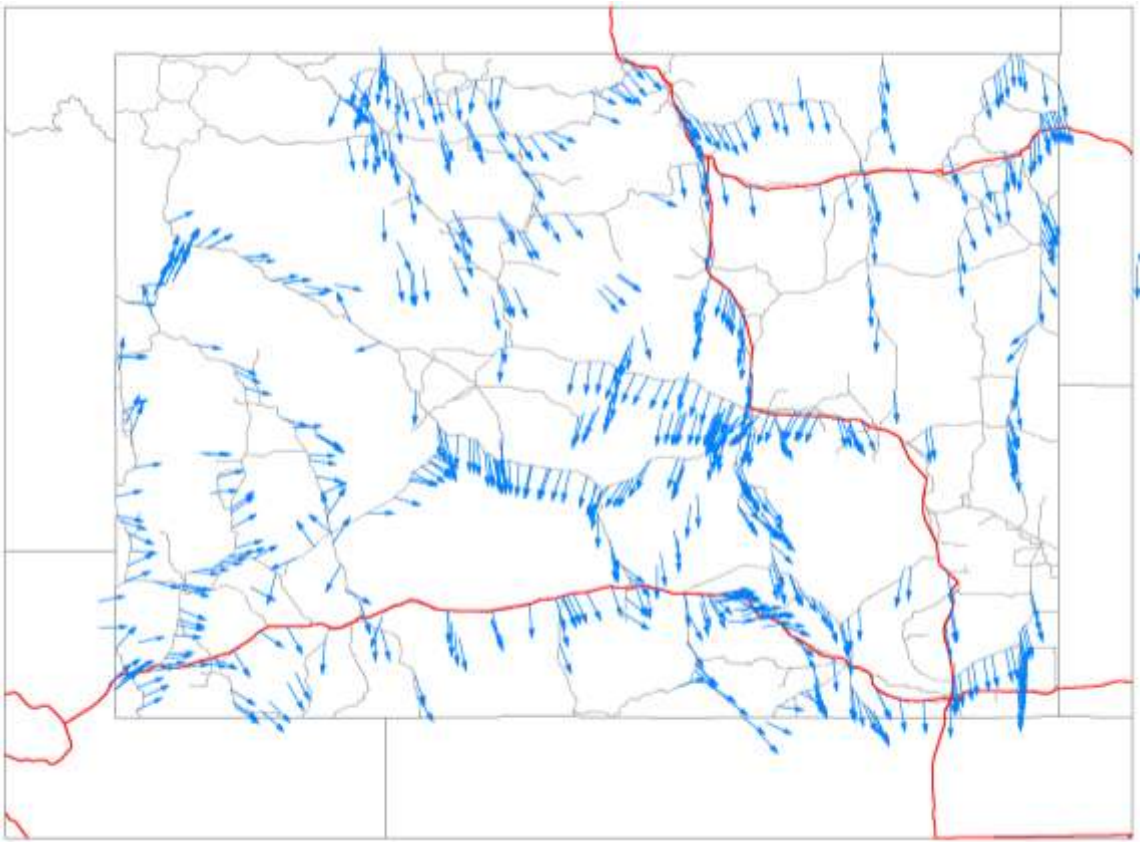

**Figure 22 Wind direction map of the winter storm period average, 1980-2014**

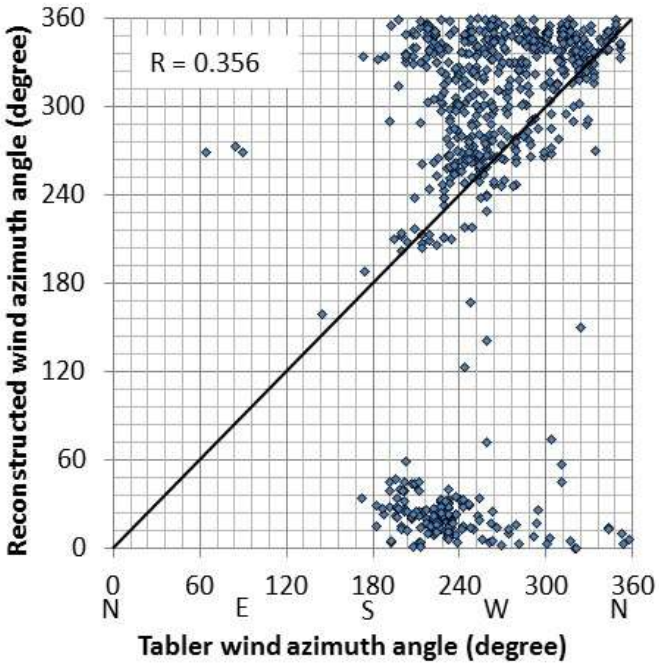


**Figure 23 - Correlation between the simulated and the observed wind azimuth angles at the data points of the Tabler data for winter storm period average 1980-2014**

***Reconstructed mean wind direction***

The average wind directions were computed at every 4 km (2.5 mi) node and converted into a GIS format. Figure 24Figure 26 visualize the final wind products for the three period averages in this project.

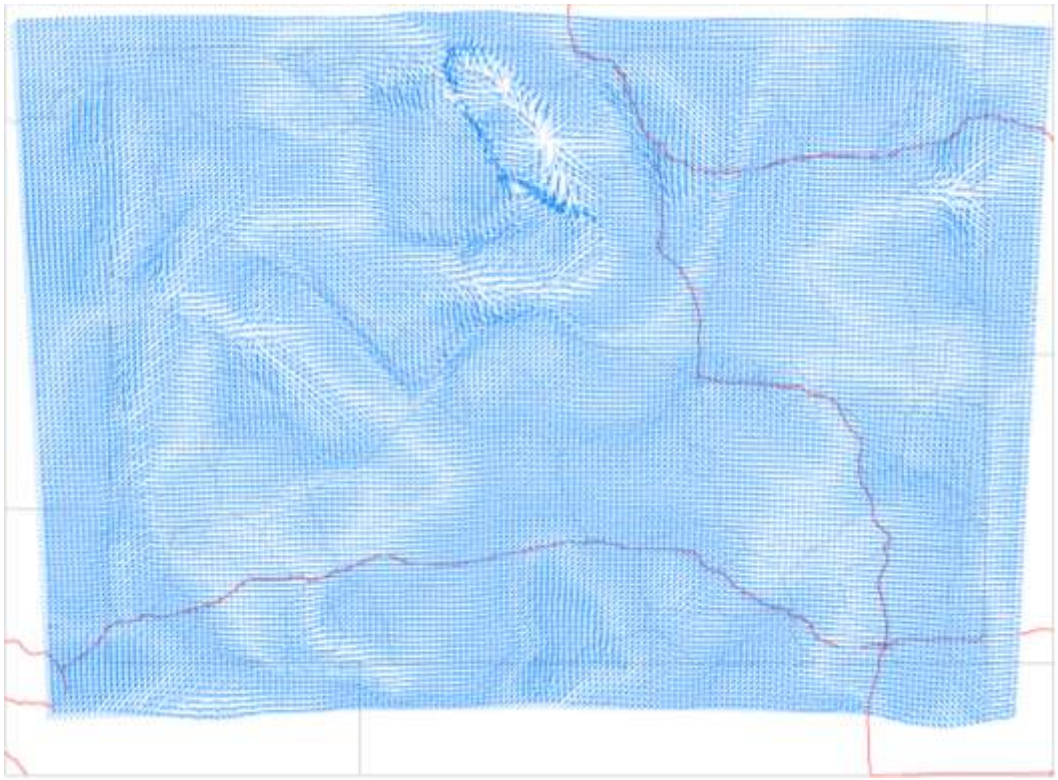

**Figure 24 - Wind direction map of the all seasons period average 1980-2014**

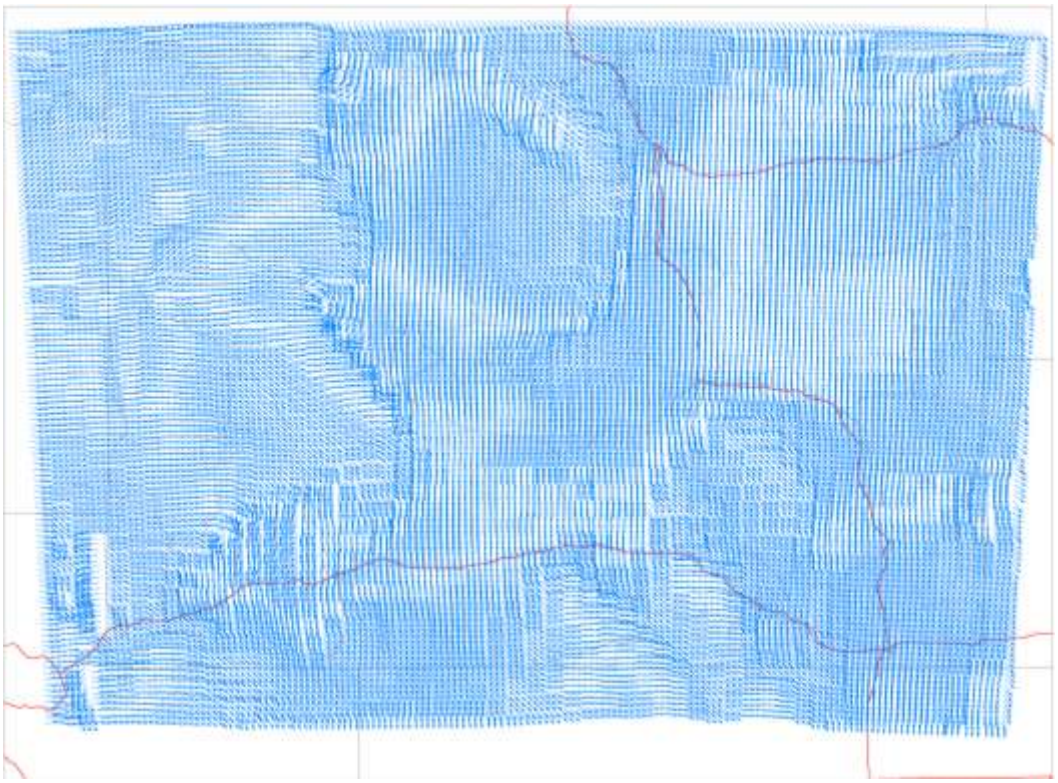

**Figure 25 - Wind direction map of the winter season period average, Oct 30th - May 1st, 1981-2014**

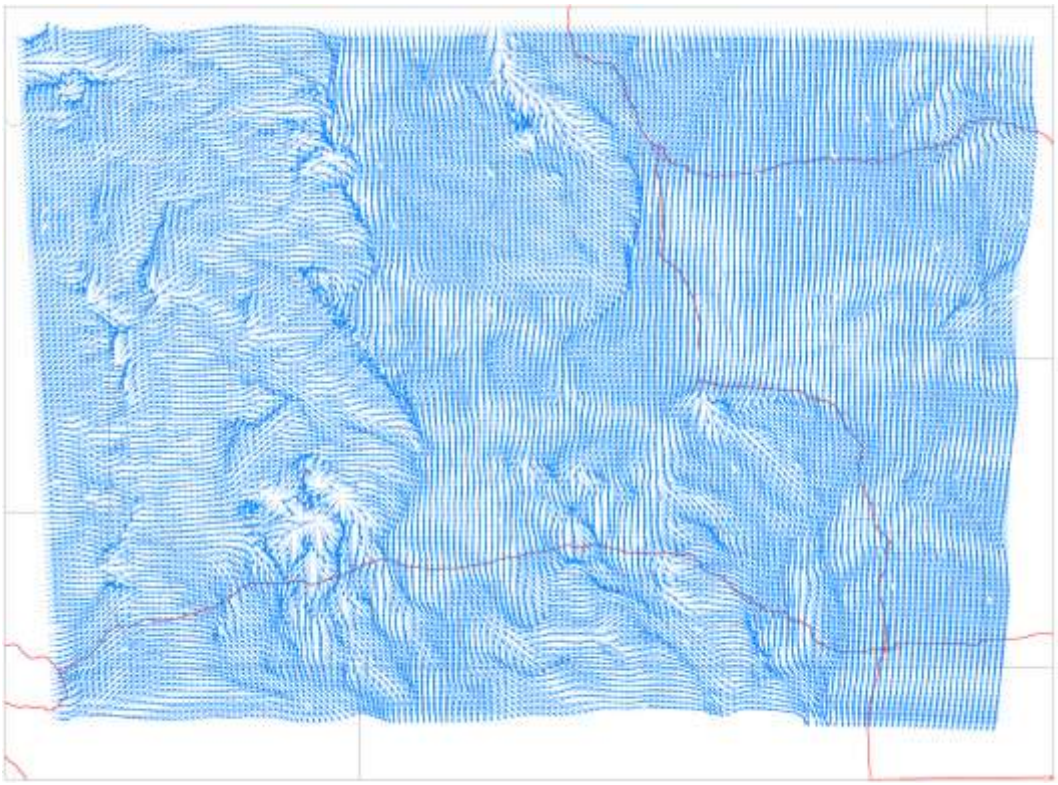

**Figure 26 - Wind direction map of the winter storm period average, 1981-2014**

***Reconstructed Standard Deviation of Wind Direction***

Similarly, the standard deviations of the wind direction were computed at every 4 km (2.5 mi) node by the Yamartino method. Unfortunately, along I-80, a major trans-continental highway for moving goods and services, many sections have a large variability in wind direction (more than 45°) making it difficult to protect these area by a single snow fence angle.

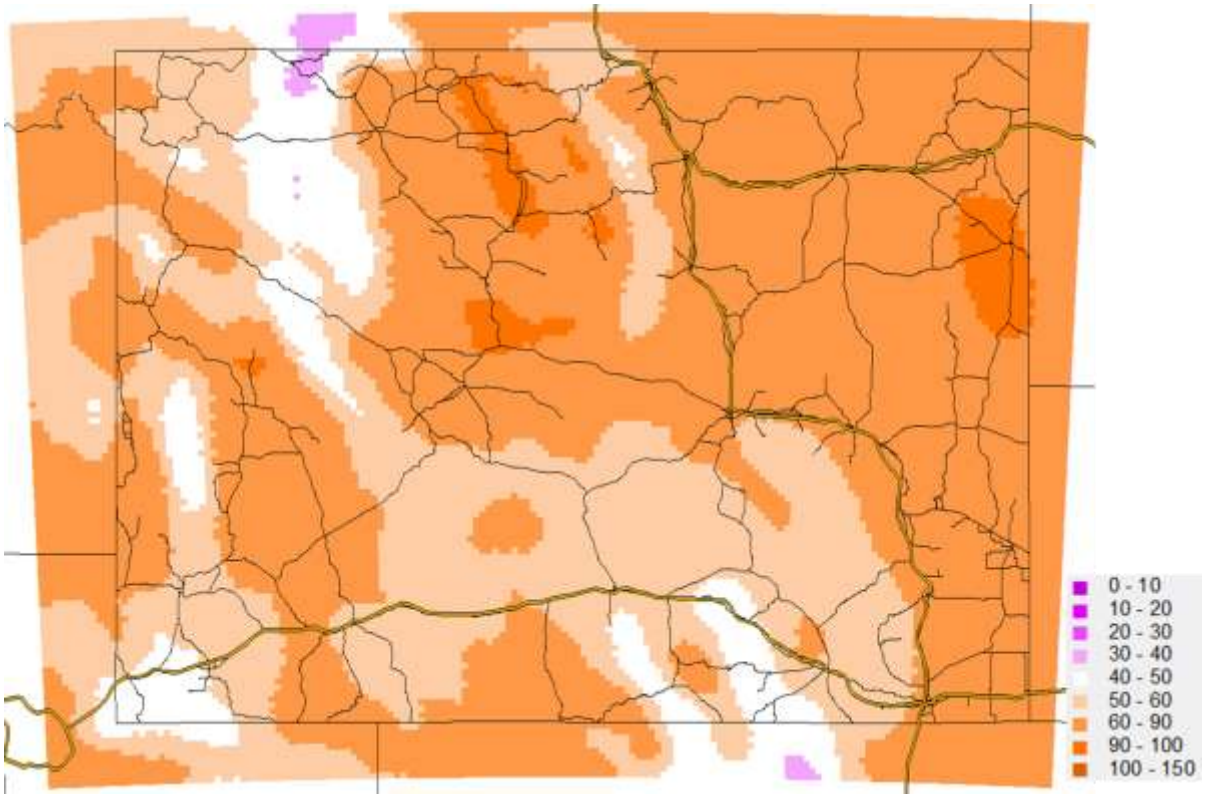


**Figure 27 – Standard deviation of the wind direction (degree) in the all seasons period, 1981-2014**

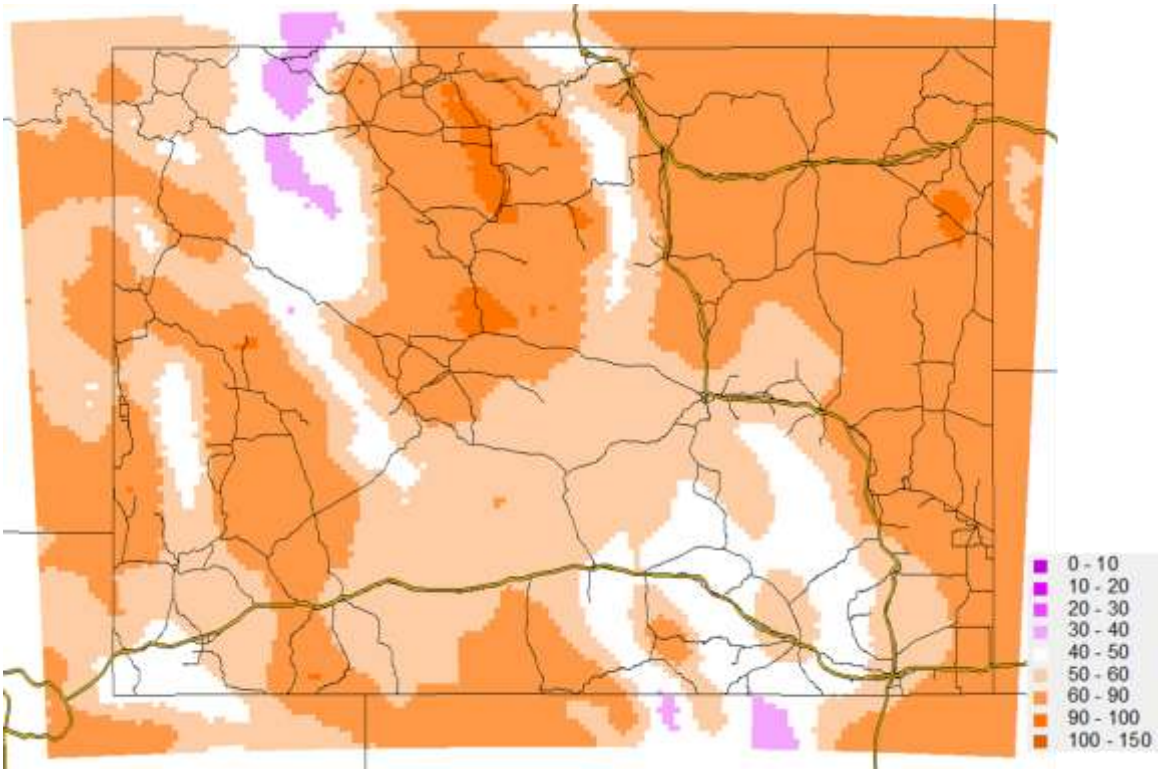


**Figure 28 - Standard deviation of the wind direction (degree) in the winter season period, Oct 30th - May 1st, 1980-2014**

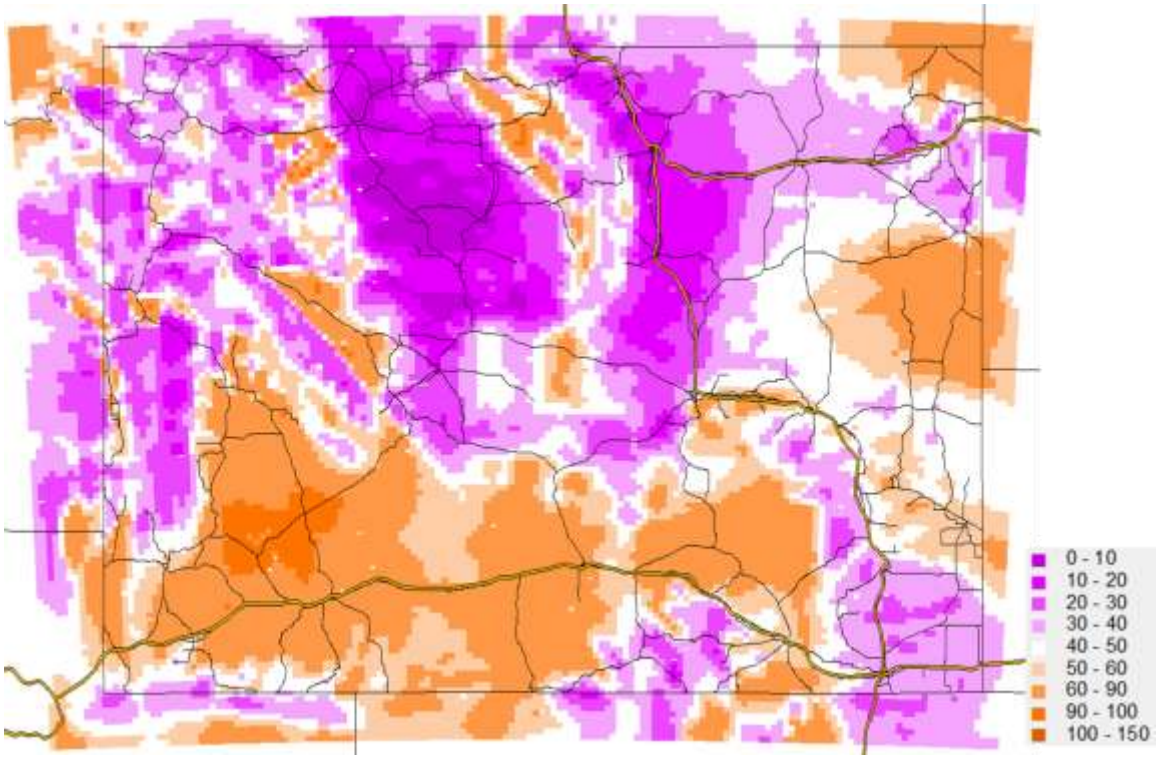


**Figure 29 - Standard deviation of the wind direction (degree) in the winter storm period, 1980-2014**

***Reconstructed wind speed***

Similarly, the average wind speeds were computed at every 4 km (2.5 mi) node for the three periods.

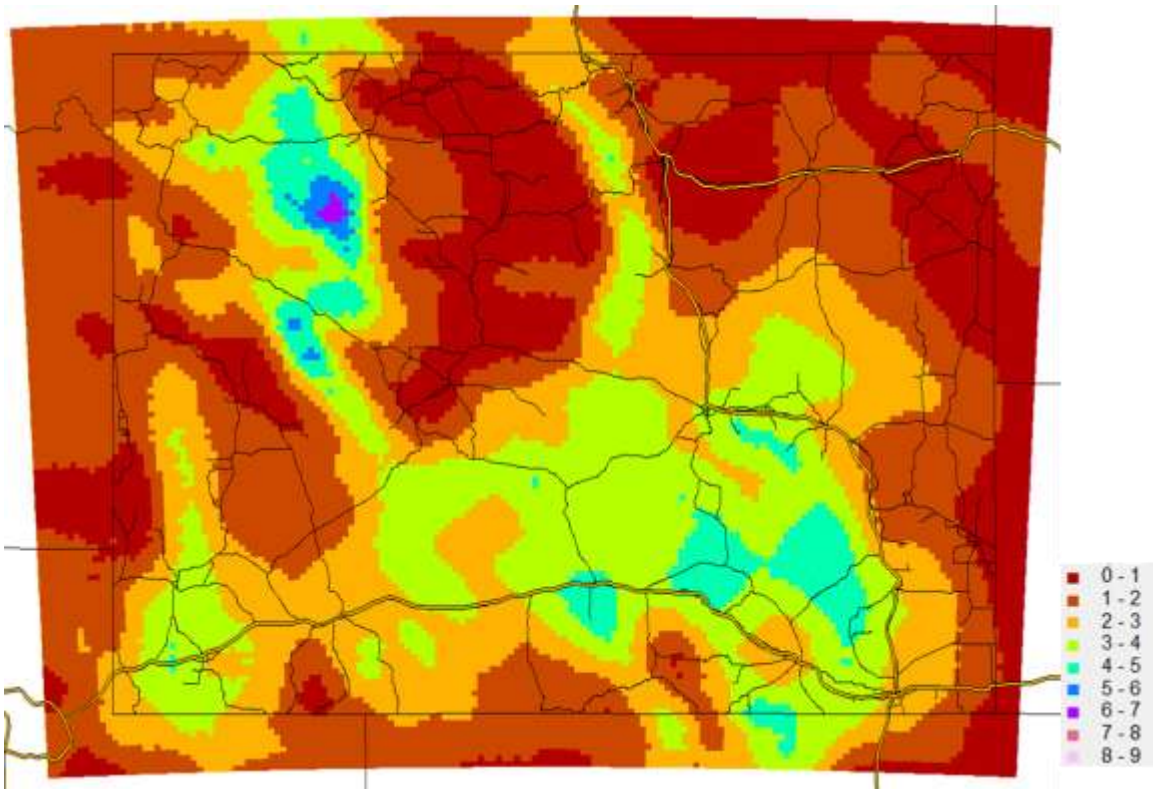


**Figure 30 - Mean wind speed (m/s) of the all season average**

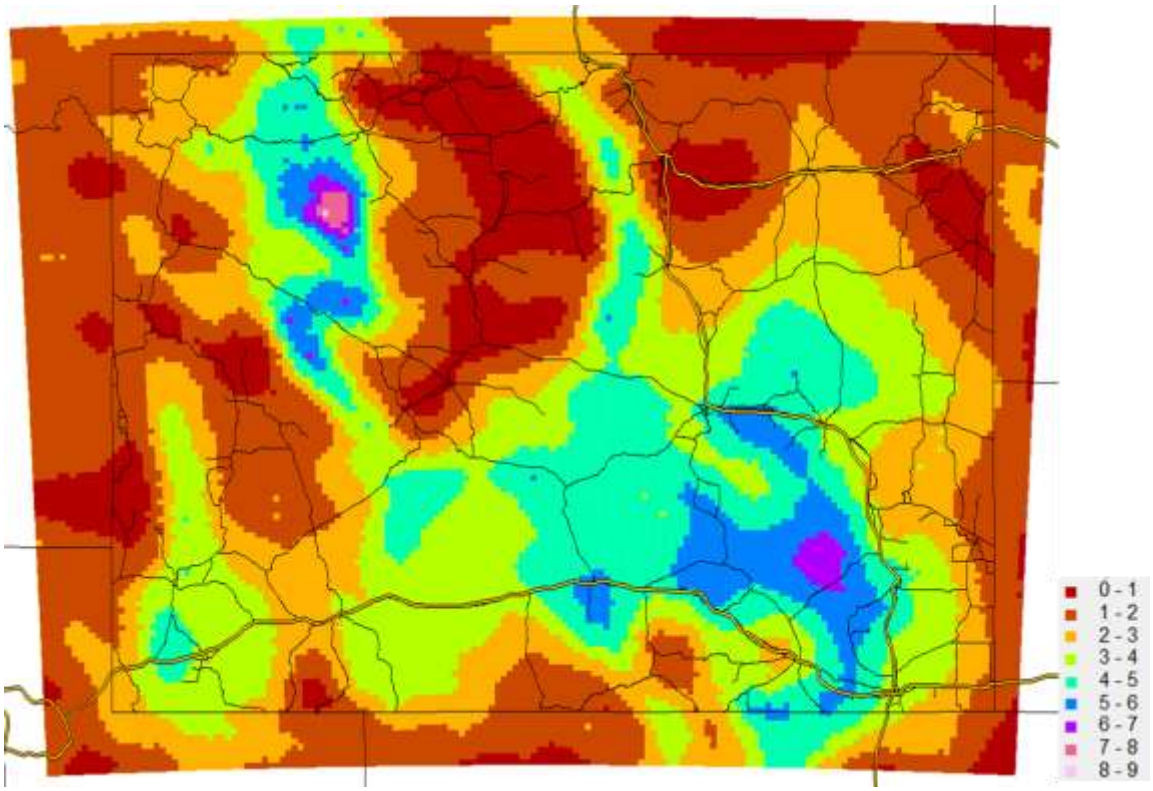


**Figure 31 - Mean wind speed (m/s) of the winter season period, Oct 30th - May 1st, 1980-2014**

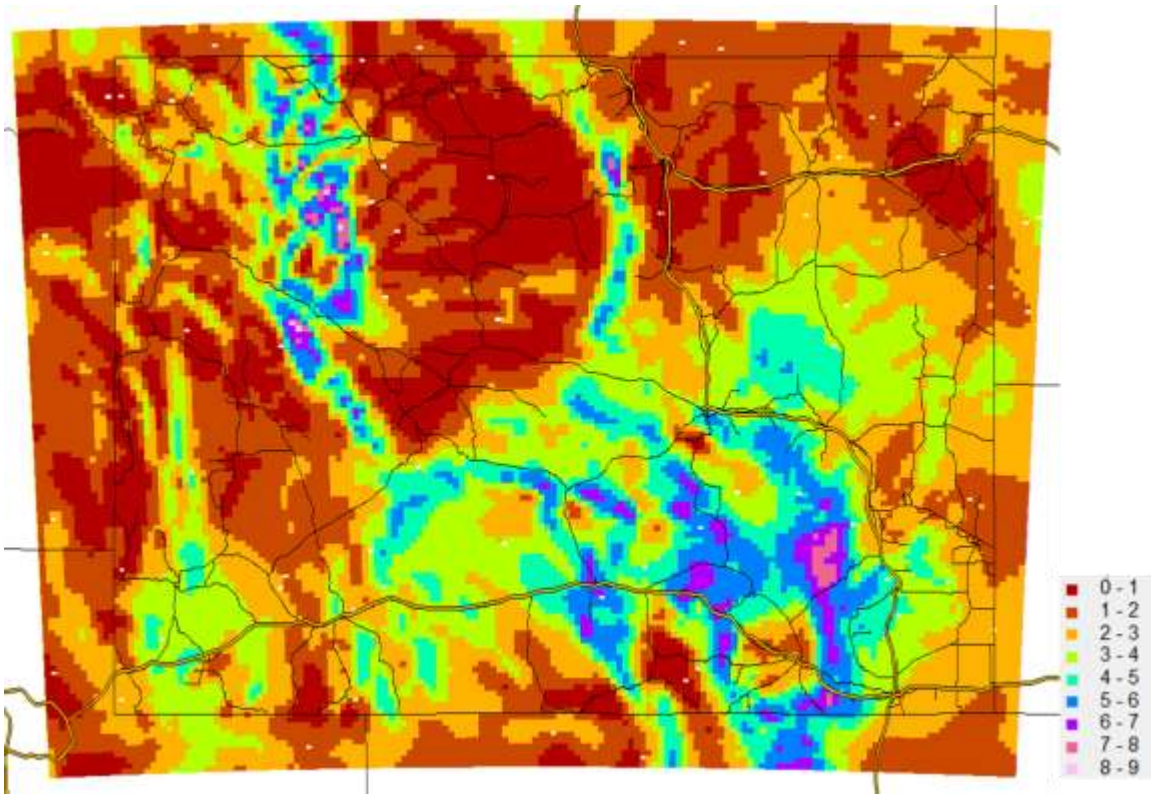


**Figure 32 - Mean wind speed (m/s) of the winter storm period, 1980-2014**

## Phase 2: Snow condition assessment

### 1) Data assimilation to existing historical records

***Acquisition of the PRISM data***

The PRISM data, which is one of the best observation-based precipitation datasets, were acquired in order to improve the accuracy of the WRF simulated precipitation. PRISM is an interpolation method developed by Daly et al. (2008), for the datasets that reflect the current state of knowledge of the spatial climate patterns in the United States. The monthly precipitation datasets were modeled using climatologically-aided interpolation (CAI), which uses the long-term average pattern (i.e., the 30-year normals) as a first-guess of the spatial pattern of the climatic conditions for a given month or day. This dataset is basically synthesized from all existing ground precipitation records in the United States by the terrain-based interpolation method (PRISM). Therefore, the PRISM data, which almost certainly reflects the real precipitation pattern in the historical period, are used as the reference precipitation dataset in this study. The total size of the dataset was about 14.2 GB in ASCII "ungenerated" format, one of the generic GIS formats.

PRISM data are consistent with the ground observed precipitation records and have a very high spatial resolution at about 4 km (2.5 mi) resolution. However, the major shortcoming of the PRISM data is the coarse, monthly temporal resolution. For accurate snowfall (snow precipitation) estimation, it is important to have at least hourly data collection. The numerical weather prediction model is less accurate in precipitation prediction compared to other atmospheric variables such as temperature, wind field, etc. Consequently, the objective of this task was to combine the simulated and observed precipitation datasets to achieve accurate seasonal, total snow precipitation estimates.

***Data assimilation***

The assimilation program was written both for the Windows and Linux environments. The precipitation data assimilation involves time and space interpolations in order to make the observed and simulated values comparable, as shown in Figure 33.

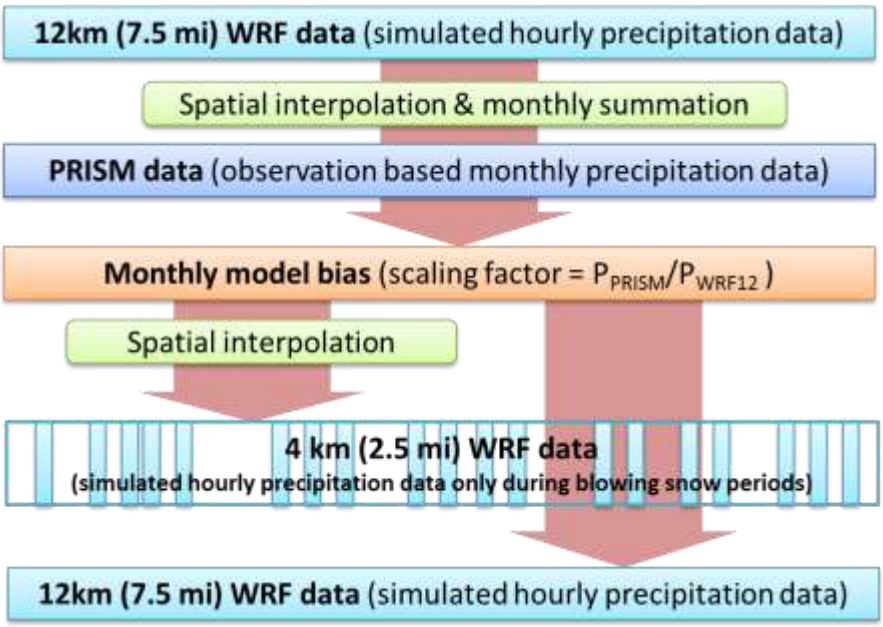


**Figure 33 - Flowchart of the precipitation data assimilation procedure**

The data assimilation was performed by taking the following steps.

1. The total monthly precipitation was computed from the WRF model outputs at every computational node for the period 1980-2014.
2. The observation-based monthly precipitations at the WRF computational node locations were computed from the PRISM data by using the inverse distance method.
3. The scaling factors of the simulated and observed monthly precipitations were computed for every computational node for every month during the 1980-2014. Note that the scaling factors were limited between 0.5 and 5.0 to avoid the outrageous precipitation totals especially in arid areas during dry seasons.
4. The spatially-distributed monthly scaling factors were then applied to the original hourly WRF simulated precipitation data. The assimilated WRF precipitation data are referred to as the bias-corrected data hereafter.

Thus, the observed and simulated monthly total precipitations are consistent while the bias-corrected simulation data has one-hour temporal resolution. An example of WRF simulated monthly precipitation fields with and without the data bias correction is shown in Figure 34. The simulated precipitation field (shown in squares) is laid over the background map, which is the corresponding PRISM precipitation field (observation). The assimilated WRF precipitation field resembles the observed precipitation field. The WRF simulation outputs near the model boundary (outside of Wyoming) are not effective for the snowfall estimation due to known interpolation artifacts of the boundary condition. Finally, Figure 35 shows the mean annual precipitation computed from the bias-corrected (or assimilated) WRF model output. This bias

corrected precipitation data were used for the annual snowfall estimation, which is one of the essential design parameters for the snow fence design.

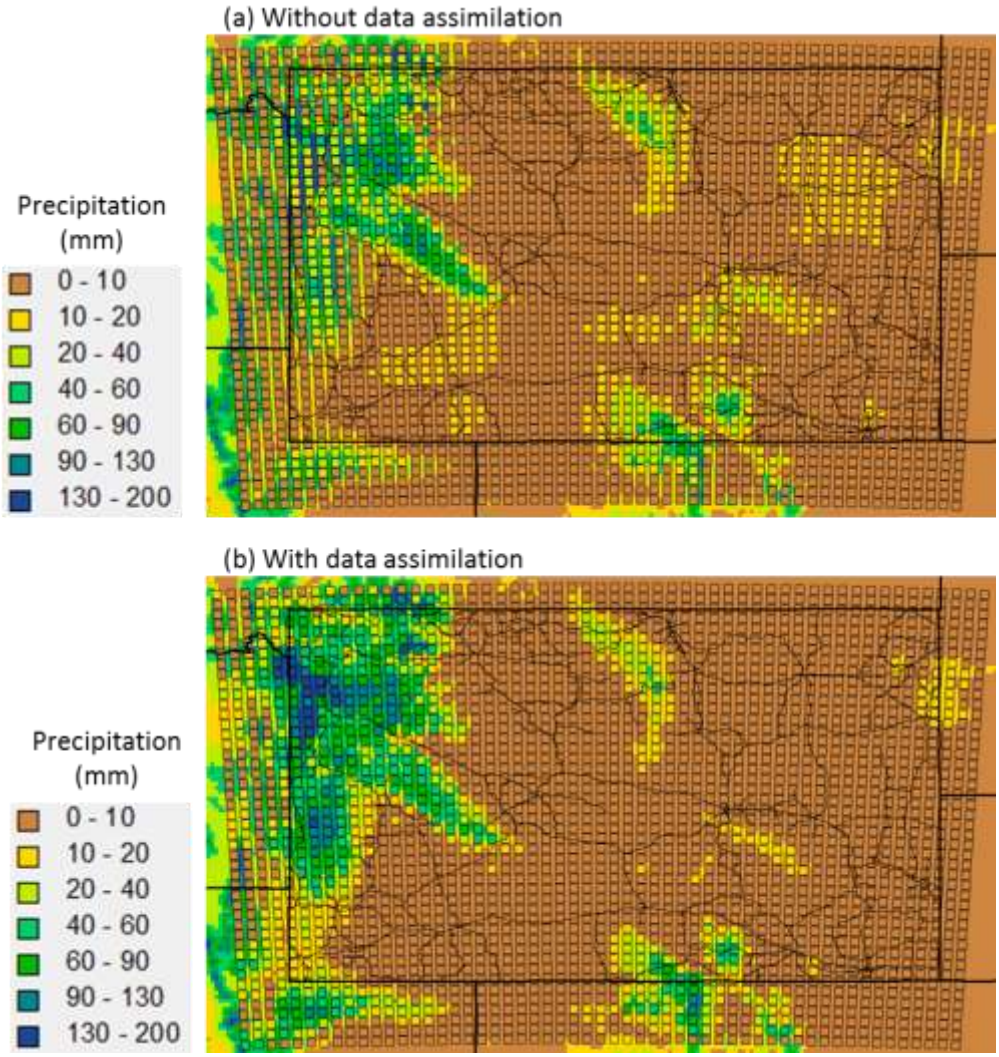


**Figure 34 - An example of the simulated precipitation field in February 1982, with and without data bias correction, superimposed over the corresponding PRISM data. The WRF simulated values are shown in squares and the PRISM data fills in between the squares.**

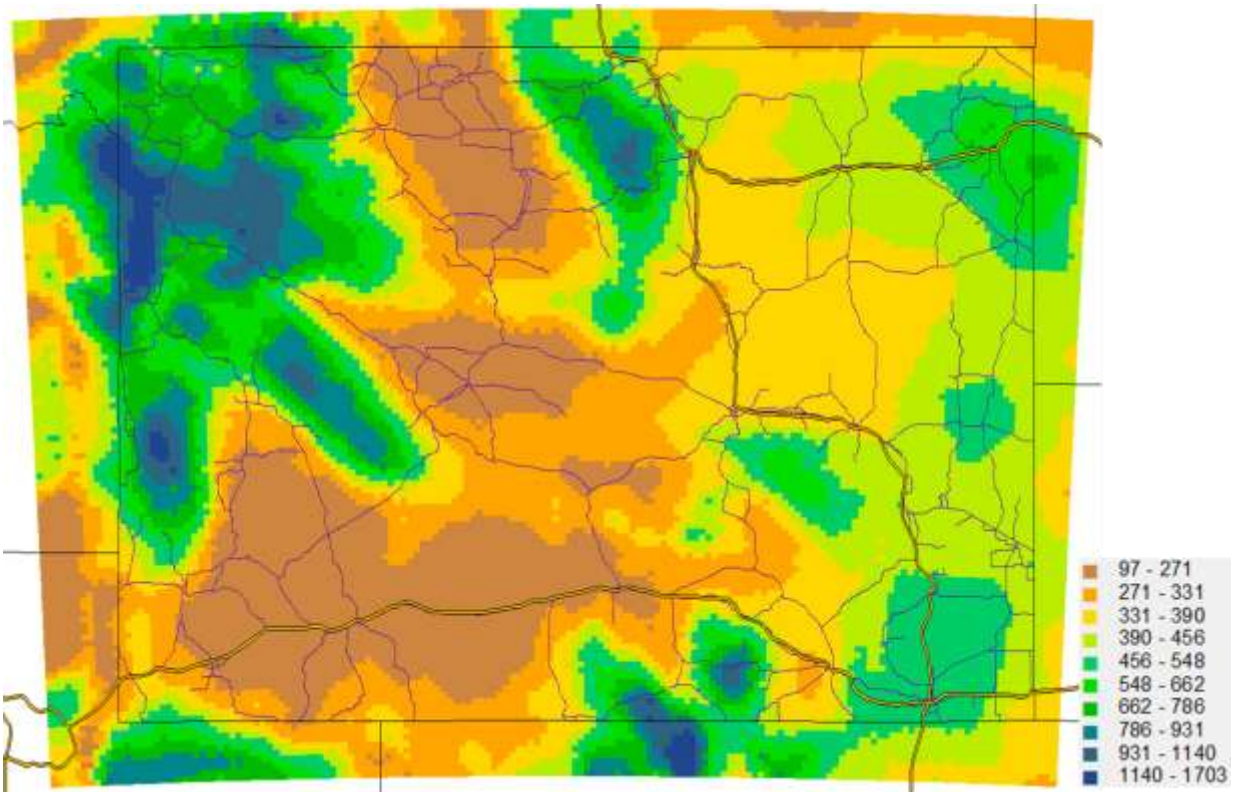


**Figure 35 – Bias-corrected mean annual precipitation (mm) in 1980-2014**

### 2) Winter precipitation data compilation for snow fence design

The snow precipitation was computed from the simulated air temperature at 2 m [6.56 feet] and the bias-corrected precipitation data at every single computational cell. The separation of the precipitation phase (snow or rain) can be performed in the atmospheric cloud microphysics modeling. However, the separation using the near surface air temperature is typically more reliable than the current parameterization due to considerable uncertainties in the atmospheric processes. Therefore, when simulated air temperature was below -1 °C [30.2 °F] (calibrated value), precipitation is regarded as snow in this study. The computed mean annual snowfall in Wyoming is visualized in Figure 36. The Tabler snow data was superimposed (square) over the simulated snowfall map using the same color scheme. Figure 37 also shows the comparison graph of the WRF simulation and the Tabler data. Clearly, the WRF simulation successfully reproduces the historical annual snow precipitation with a high correlation coefficient. At a minimum, the bias-corrected WRF estimation of annual snowfall seemed an excellent interpolation of the field-observed snow data using an all process-based understanding of the atmospheric processes over complex terrain.

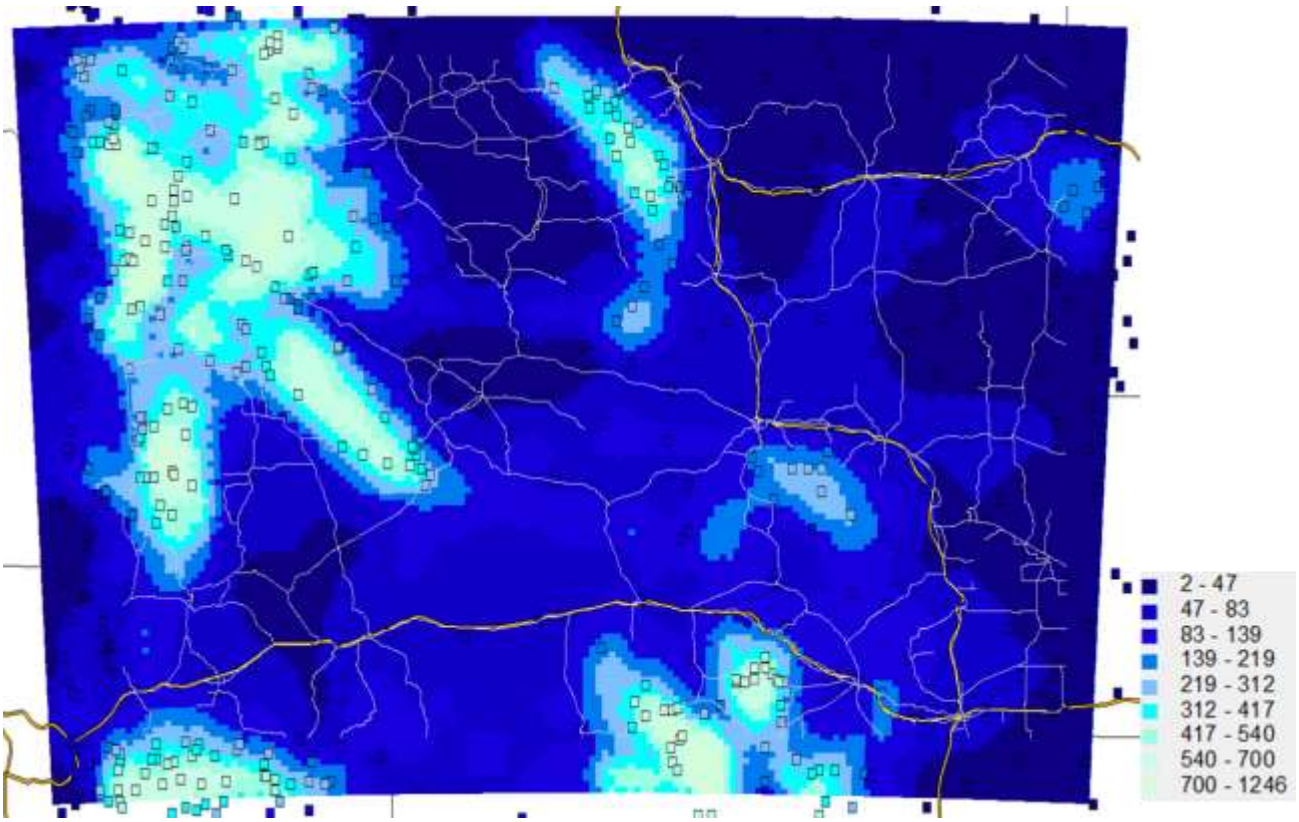


**Figure 36 – Computed mean annual snowfall (mm/year) in 1980-2014 and the Tabler data in squares**

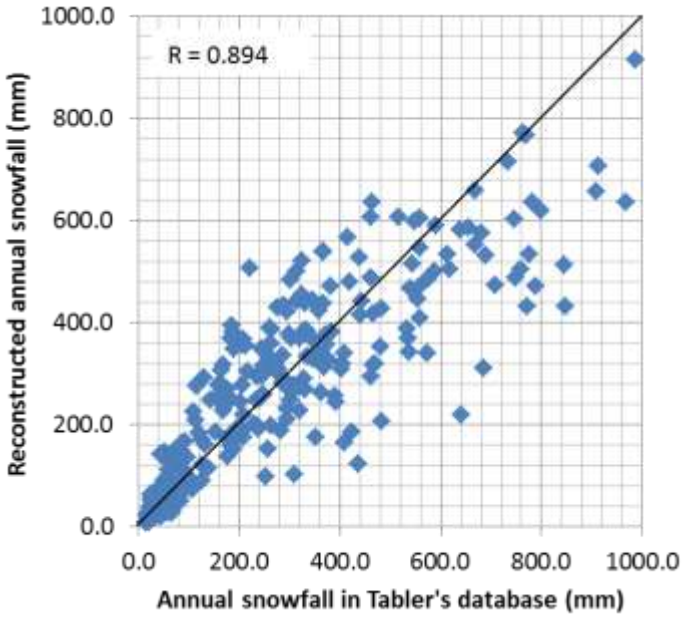


**Figure 37- Validation of the simulated annual snow precipitation with the Tabler data (snow courses, snow pillows, and precipitation gauges)**

Figure 38**Error! Reference source not found.** shows the time series of the simulated monthly precipitation and snowfall in Wyoming. This graph suggests a very small to no trend (+0.048 mm (0.002 in) per decade) in the snowfall in Wyoming. Figure 39**Error! Reference source not found.** shows the simulated monthly mean air temperature in Wyoming. According to the linear trend line, the climate of Wyoming has clearly gotten warmer over the last 34 years (+0.3 °C (0.17 °F) per decade). It is interesting that the temperature change effect on the annual snowfall has not been prominent due to the complex nature of precipitation-generating processes over Wyoming.

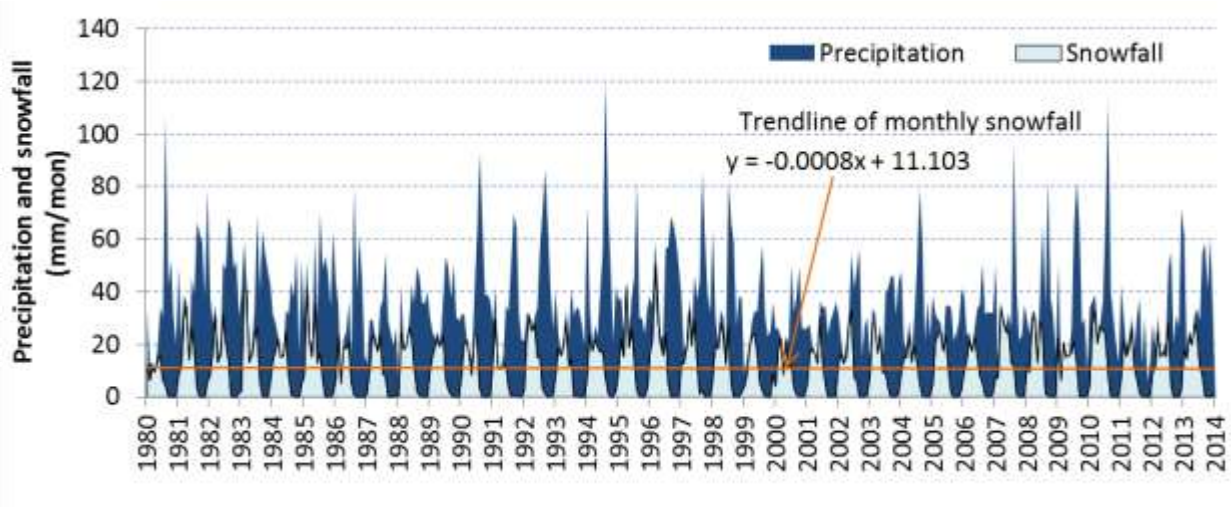


**Figure 38 - WRF simulated monthly precipitation and snowfall (Wyoming average) in October, 1980 – September, 2014**

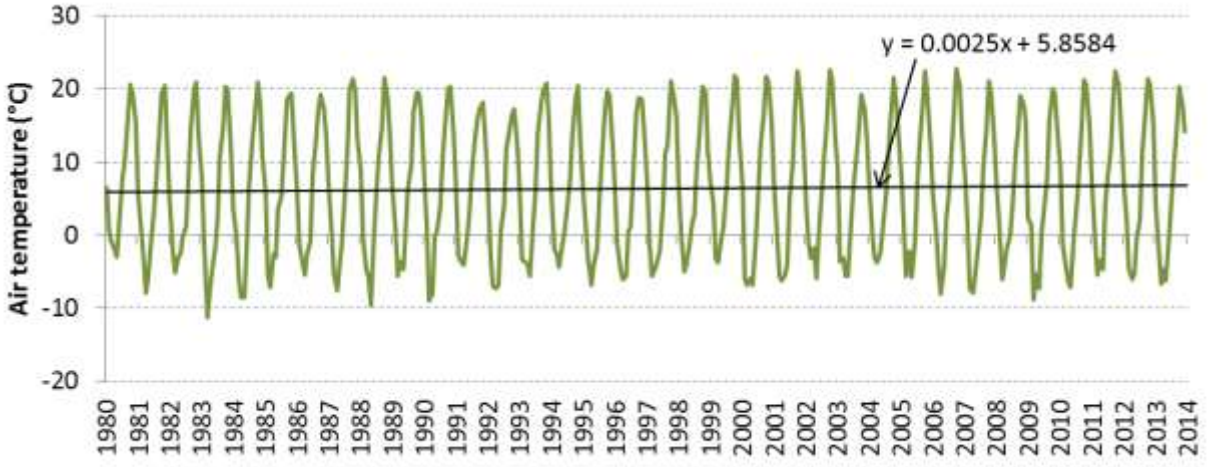


**Figure 39 - WRF simulated monthly mean air temperature (Wyoming average) in October, 1980 – September, 2014**

***Characterization of extreme blowing snow events in Wyoming***

The blowing snow risk was assessed using the WRF simulation outputs based on the methodology developed in Phase 1, task 3, modeling of mobile and blowing snow. The blowing snow depth was computed from the bias-corrected, hourly snow precipitation, air temperature, and wind speed at every computational node of the 4 km (2.5 mi) grid system. The blowing snow risk is defined as the frequency of the blowing snow depth greater than 1 mm (0.039 in) in this study. The blowing snow risk in 1980-2014 is visualized in Figure 40. This figure shows the significant spatial variability in the blowing snow events along I-80 in Wyoming. Mewes (2011) also estimated the blowing snow hours in the United States combining the NAM model and a simple snowmelt model during 2004-2005; his estimates were quite comparable although his definition of blowing snow was different from that used in this study. Note that the number of days was computed as a summation of the blowing snow hours. Therefore, the corresponding road closure periods may be longer than the computed blowing snow periods. Also, there are no systematic blowing snow observation data to check the model-based estimation. However, many of the known blowing snow sections are delineated by this model-based risk map in Figure 40. This high resolution blowing snow risk map may be useful for optimization of the winter maintenance resource distribution, as well as for improvement of the snow fence system.

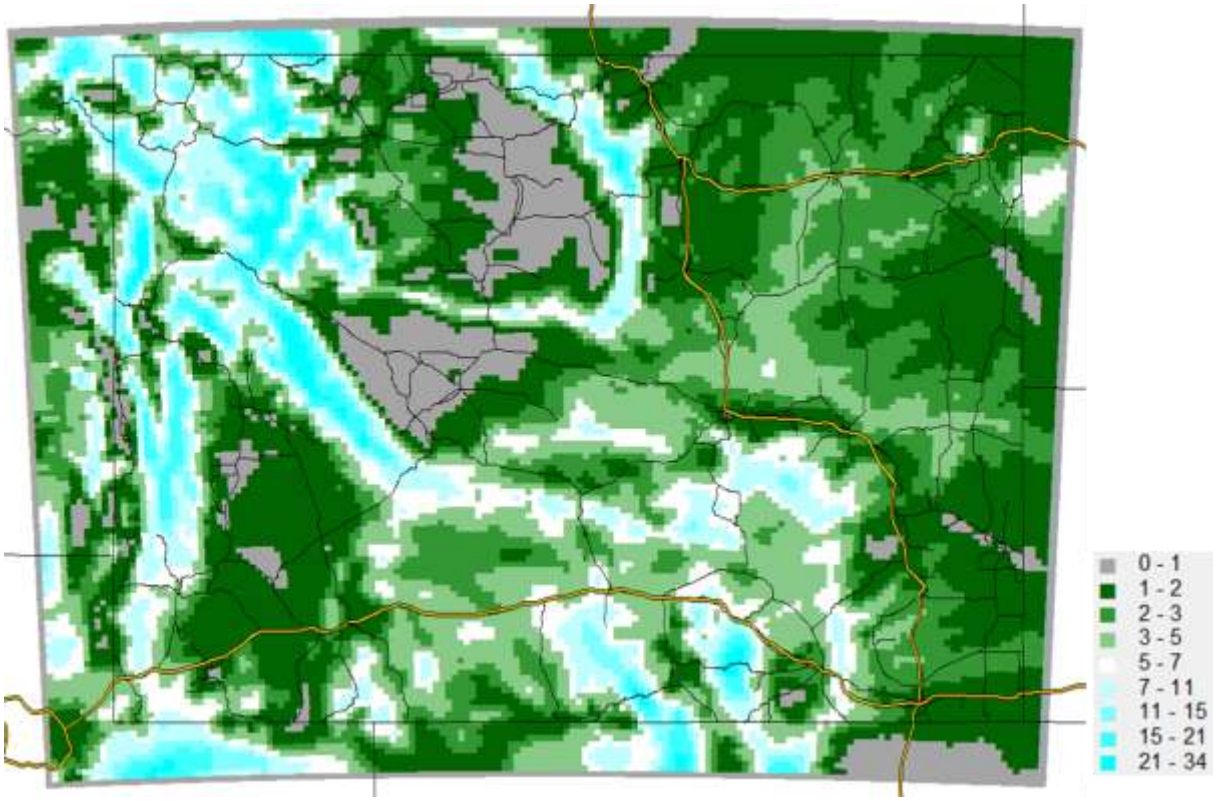


**Figure 40- Computed average number of blowing snow days per year (1980-2014)**

A long-term trend analysis of the blowing snow occurrences was also performed based on the reconstructed climate data in Wyoming. The number of days that had more than 1 mm (0.039 in) of blowing snow were computed at every five year period from 1980-2014 (Figure 41). The analysis suggested that recently Arlington, WY, where the original snow fence study took place, had a few more potential blowing snow periods than in the 1980s. According to the wind simulation using the WRF model with NARR data, the blowing snow risk for Arlington, WY, increased over the last three decades.

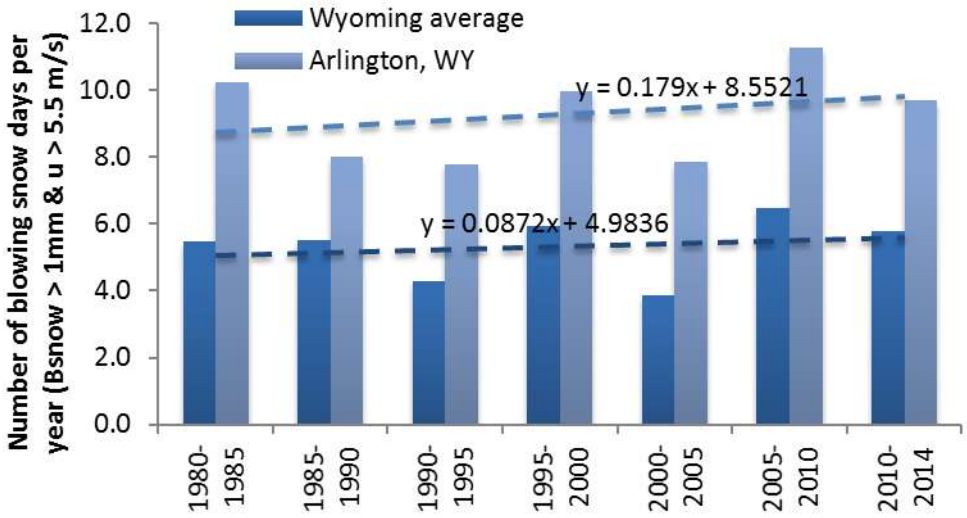


**Figure 41 - Blowing snow days statistics in Wyoming and at Arlington, WY, during the last three+ decades based on the reconstructed weather condition**

According to Figure 41, the blowing snow risk trended slightly upward in last three decades (+0.36 days per decade for Arlington, WY, and +0.17 days per decade for Wyoming average), although the occurrence varied from half decade to half decade. This is mainly due to the increasing trend in wind speed (Figure 13) with nearly constant snow precipitation (Figure 38) throughout the simulation period. Although the temperature in Wyoming had a clear upward trend under the changing climate in this simulation (Figure 39), it may have been just cold enough to have snow precipitation. Therefore, the blowing snow risk in Wyoming has not decreased in the last 34 years due to the climate change. Even though the blowing snow risk may be mitigated by temperature increase in distant future, it may be wise to pay more attention to the blowing snow hazard today and in near future.

***Change in wind directions***

Figure 42Figure 43 show the wind azimuth angle comparisons in scatter charts for three decades: 1980, 1990, and 2000. Figure 42 shows the change in the all seasons period average wind directions, and Figure 43 shows the change in the winter storm period average directions. The graphs show almost no change in the wind direction over the last three decades, neither by all-season nor winter storm period averages.

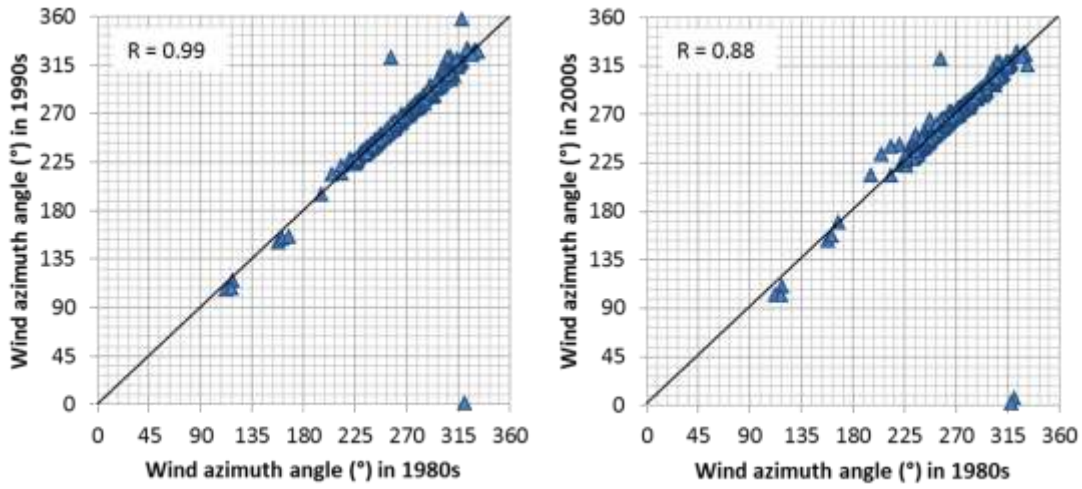


**Figure 42 - Wind azimuth angle comparisons for all season period average among 1980s, 1990s, and 2000s. Each point represents location of the Tabler data.**

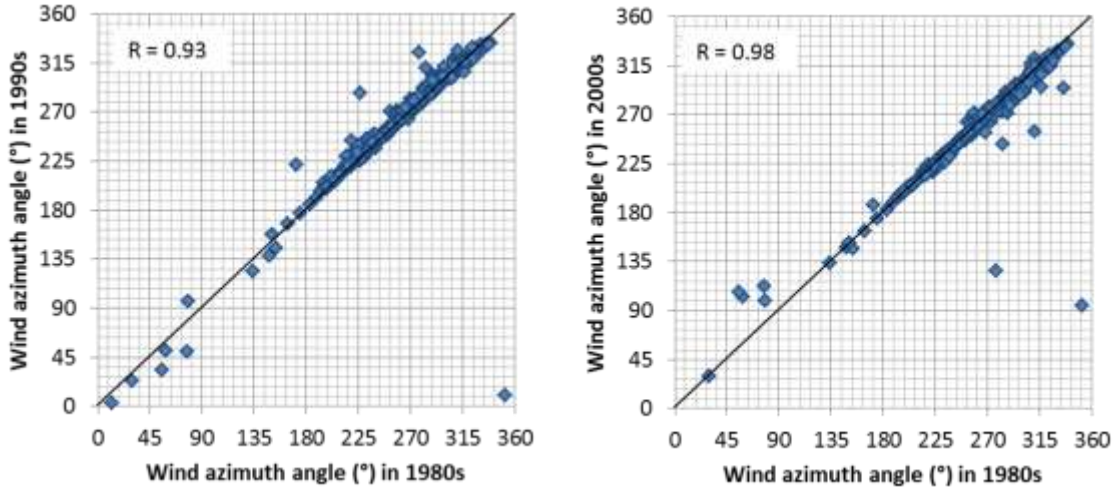


**Figure 43 - Wind azimuth angle comparisons for winter storm period average among 1980s, 1990s, and 2000s. Each point represents a location of the Tabler data.**

# CHAPTER 4 PRODUCTS

## 4.1 Data

The following data products were submitted to WYDOT.

1. Wind and snow statistics produced by the WRF model with the NARR data for 1981-2014 at 4 km (2.5 mi) grid (20412 points).
2. Wind and snow statistics produced by the WRF model with the NARR data for 1981-2014 at the Tabler wind data points (694 points).

Items 1 and 2 contain following variables:

a. ST_ID = Sequential number.
b. LON(DEG) = Longitude.
c. LAT(DEG) = Latitude.
d. ELV(M) = Elevation (m).
e. PREC_ANNUAL(mm) = Average annual precipitation for the entire 1980-2014 period.
f. SNOW_ANNUAL(mm) = Average annual snowfall for the entire 1980-2014 period.
g. Tabler_Azimuth(Deg) = Wind azimuth angle in Tabler's table (Tabler table only).
h. Sim_all_Azimuth(Deg) = Average wind azimuth angle for the entire 1980-2014 period.
i. Sim_all_SD(Deg) = Standard deviation of wind azimuth angle for the entire 1980-2014 period.
j. Sim_winter_Azimuth(Deg) = Average wind azimuth angle during winter months (Oct 30$^{th}$ – Apr 1$^{st}$) in the 1980-2014 period.
k. Sim_winter_SD(Deg) = Standard deviation of wind azimuth angle during winter months (Oct 30$^{th}$ – Apr 1$^{st}$) in the 1980-2014 period.
l. Sim_storm_Azimuth(Deg) = Average wind azimuth angle during winter storm period in 1980-2014 period (= bsnow period in progress reports).
m. Sim_storm_SD(Deg) = Standard deviation of wind azimuth angle during winter storm period in 1980-2014 period (= bsnow period in progress reports).

## 4.2 Dissemination and implementation

Dissemination and implementation of the products will be through statewide, national, and international sources. This research will be entered into the TRID, Transportation Research Information Database, maintained by the U.S. National Academies Transportation Research Board, with sponsorship from State Departments of Transportation where it will have national and international availability. The research and data will also be made available through the National Research Library, FHWA, the Wyoming State Library, the Wyoming State Climate Office, and other meteorological agencies working within the state of Wyoming to provide much needed statewide coverage.

The database created by this project will supersede the tables created by Tabler and will be incorporated into snow fence design within WYDOT programs, including Winter Research. The data is currently in the Statewide Snow Fence Inventory where it is updating ESRI ArcGIS spatial models used to predict drift formation and location, as well as, the sections of roadway protected by the snow fence. The spatial models, written in python scripts and run within ArcGIS Desktop, have the potential to evaluate snow fence performance either individually or by a series of fences along roadway segment. This project's data has also improved the quality of data output from the spatial models by using a new, state-wide, prevailing winter wind data to model each fence, and by removing the assumption that prevailing winds are perpendicular to the existing snow fences. The output of the spatial models will also be incorporated with the WYDOT Highway Safety Program's crash data to better identify the areas where highway safety may be improved with snow fence.

Additionally, the Statewide Snow Fence Inventory is shared with the Wyoming State Forestry Division who partners with WYDOT with the Living Snow Fence Program. The 34-year, continuous simulation of the prevailing winds computed in this project will assist the State Forestry Division as they maintain the fire management on state lands.

The produced data have already been incorporated in the Wyoming snow fence inventory for visualizing roadway protection and drifting. Example wind data visualizations in the inventory prepared by Trihydro Corporation are shown in Figure 44 for Arlington, WY, and Figure 45 for west of the Arlington, WY (247 milepost).

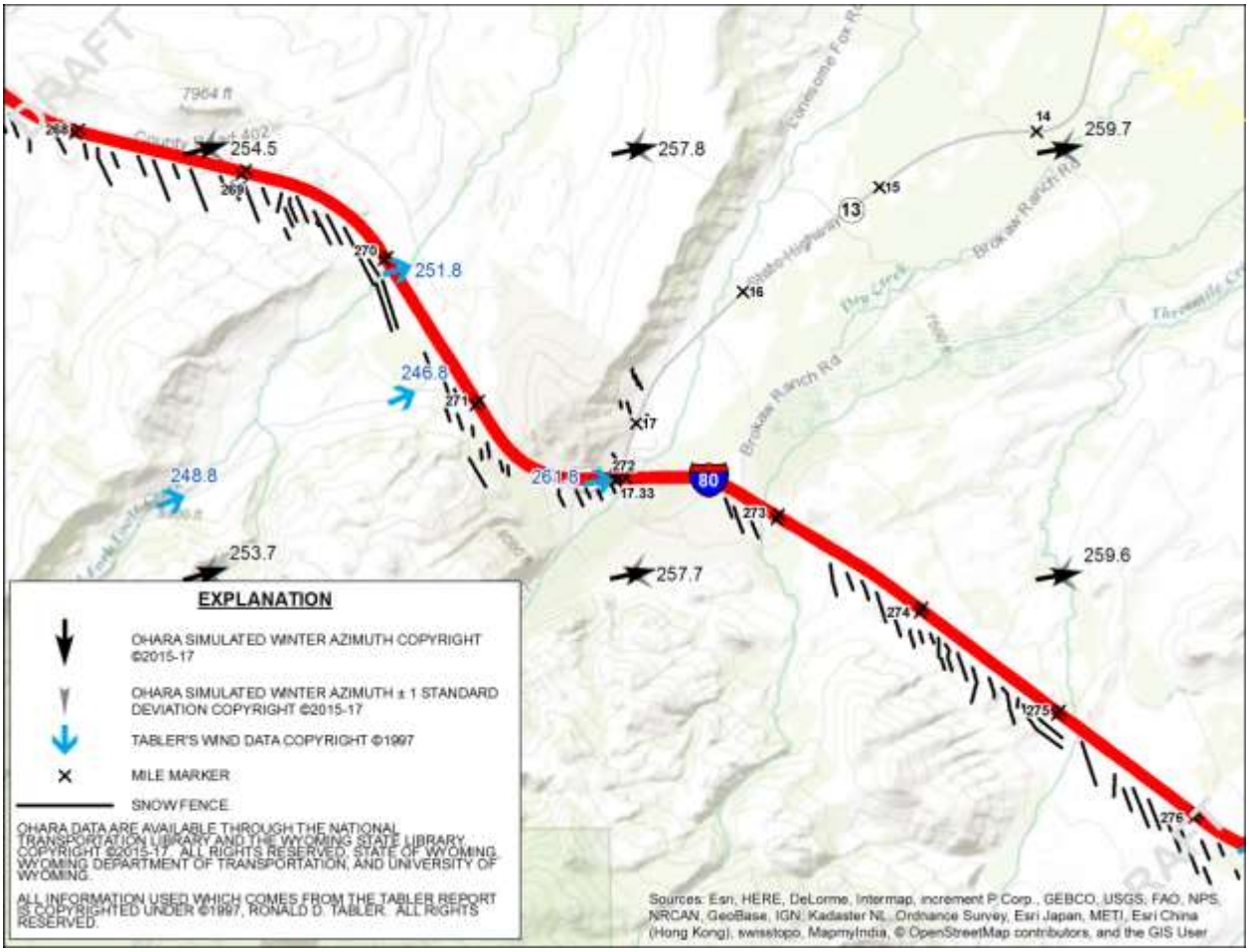


**Figure 44 - Example visualization of the Tabler data and the new simulated wind data around Arlington, WY, in the Wyoming snow fence inventory**

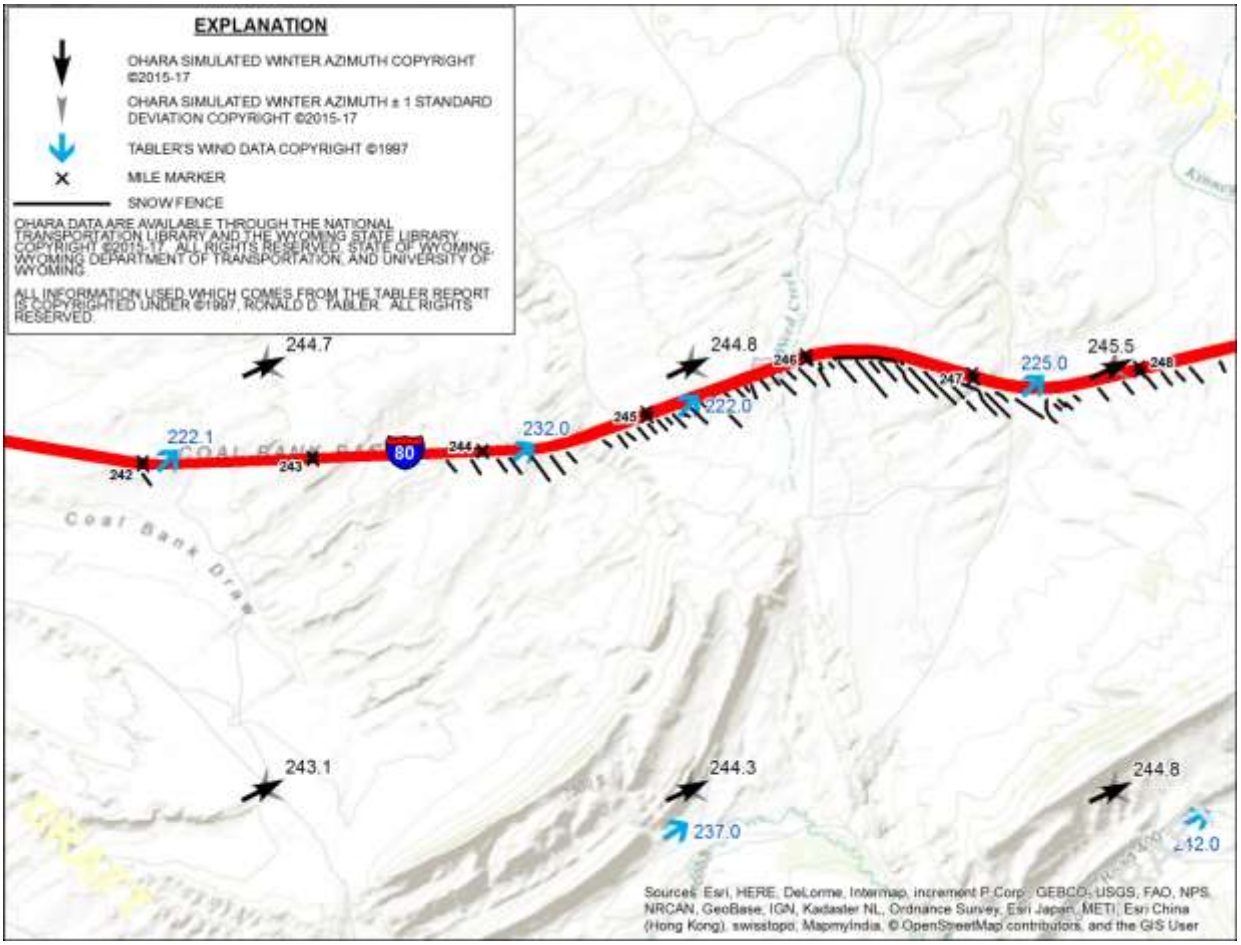


**Figure 45 - Example visualization of the Tabler data and the new simulated wind data in the west of Arlington, WY, in the Wyoming snow fence inventory**

The research outcomes have been and will be disseminated through the graduate and undergraduate programs at the University of Wyoming, as well as national and international conferences and journal publications.

1. The research outcomes of this project were presented in CE1000 VISTA studio I, introduction to civil and architectural engineering professions for freshmen, and CE2000 VISTA studio II, a first practice experience in civil and architectural engineering for sophomores, during the fall 2016 semester at the University of Wyoming.
2. Fundamental snow fence design procedure and the incorporation of the new simulation data were covered in CE5880 Advanced Hydrology, a graduate-level cold region engineering class, in the spring 2017 semester at the University of Wyoming.
3. The initial assessment of the historical weather simulations was presented in the TRB 2016 International Conference & Workshop on Winter Maintenance and Surface Transportation Weather, April 25-27, 2016, at Fort Collins, Colorado. The presentation

was titled, “Evaluation of Winter Weather in Wyoming Based on Numerical Weather Modeling for Snow Fence System Design”.

4. The final products were presented in the 2017 TRB Annual Meeting, Washington D.C. The presentation title was, “Reconstructed Historical Wind Field for Winter Weather Hazard Mitigation in Wyoming Using Weather Research and Forecasting Model”.
5. A peer reviewed journal publication is planned.

# CHAPTER 5 CONCLUSIONS AND RECOMMENDATIONS

## 5.1 Summary

Prevailing wind field and snow precipitation data are essential information for winter weather preparation including snow fence system design. However, it is difficult to obtain data under adverse winter storm conditions in remote areas. This study provided an alternative method using a numerical model-based data through dynamic downscaling of NARR data using the WRF model.

First, the coarse resolution simulation at 12 km (7.5 mi) resolution was validated by using the wind record (SCRAM data) at airport sites in terms of wind statistics. The WRF-simulated wind field is realistic enough for blowing snow risk assessment in this region and it updated the Tabler data. The blowing snow periods were identified based on this 12 km (7.5 mi) WRF simulation during the period of 1980-2014. The fine resolution WRF simulation at 4 km (2.5 mi) resolution was implemented during the identified blowing snow periods. The simulation covered nearly 500 winter-condition weeks encompassing most of the blowing snow periods. This fine-resolution model provided more accurate and localized blowing snow risk assessment.

The analysis using the WRF simulation indicated that Wyoming has become significantly windier during the last 34 years. It is unknown whether or not this trend can be extrapolated toward the future. However, it is wise to pay attention to wind-related hazards in Wyoming. The continuous and complete weather simulation data enabled the identification of the blowing storm periods. The number of blowing snow events have increased slightly in last three decades due to increased wind speed. Wyoming has had persistent blowing snow even under the recent climate changes.

The simulated prevailing wind direction map during the winter season (October - May) was found to be consistent with the existing manually-collected wind data by Dr. Tabler. Therefore, the existing snow fence system is considered to be effective for average wind conditions over the winter season. However, the simulated wind pattern during the winter storm events was found to be quite different from the prevailing wind maps during all seasons and the winter season. Moreover, the deviations of the wind direction were found to be very large along the I-80 corridor (more than 45 degrees). Knowing that the snow fence performance depends on the relative snow fence angle to the wind direction, it may be possible to improve the efficiency of the fence system by incorporating the simulated wind statistics.

The bias-corrected snow precipitation was prepared for new snow fence sizing. The new snowfall data that were produced by the WRF model and the PRISM data showed agreement with the Tabler data derived from snow course, snow pillow, and precipitation gauges. This model-based dataset should have better accuracy than the simple spatial interpolation of the Tabler data points. Combining the dynamic wind fields and the high-resolution snow

precipitation data, the blowing snow risk has been quantified in terms of the annual blowing snow days in Wyoming.

Finally, this project provides better data to design snow fence in areas where wind and precipitation data are hard to obtain. By maintaining this dataset it is possible to better focus winter maintenance strategies in areas of high winds and blowing snow. The model-based fundamental wind and snow data can be used for snow fence improvements, maintenance, and new strategies. The reconstructed wind fields, with complete spatial coverage in Wyoming, are clearly useful to assess travel risks under the adverse weather conditions and potentially to improve the snow fence system given the evolving climate.

## 5.2 Recommendations

The immediate recommendation is local snow fence performance assessment based on the complete wind statistics from the WRF simulation, especially for the frequent blowing snow areas (Figure 40). For example, the protected time frequency by snow fence along the major freeways should be useful for identification of the most vulnerable road sections.

Further model validation with the Road Weather Information System (RWIS) data will assure the confidence level of the model-based weather data. This project validated the model outputs for the state-wide scale for the long term (34 years) and did not directly test them using the local surface observations. Additional continuous fine resolution simulations in the recent years (after 2010) would provide more opportunity for direct comparisons and possibly data assimilation.

Suggested update frequency of the fundamental weather data is 5-10 years, depending on how fast climate change affects the weather system in Wyoming. According to the trend analysis, the decadal update seemed sufficient for the last three decades. However, the widely accepted emission scenario in the Intergovernmental Panel on Climate Change (IPCC) (Nakicenovic et al., 2000) suggested that climate change may be accelerating.

A scientific climate change study based on the current General Circulation Model (GCM) projections would be desirable to allocate the state resources efficiently. If the climate warms further, the blowing snow risk would reach a maximum and eventually decline. The atmospheric and hydrological responses to the climate change are very complicated, and different kind of hazards may emerge in the future. The early preparation for the tipping point of winter weather regimen is certainly beneficial for the road management agencies such as WYDOT.

**Acknowledgments:**

This study was funded by the Federal Highway Administration (FHWA) FHWA-WY-17/03F, and executed as the Wyoming Department of Transportation, Grant No. RS06215**.**

The data generated under this project were dependent on several public-domain resources as explicitly noted throughout this final report. They include the WRF-ARW model (version 3) and NARR dataset by the National Centers for Environmental Prediction (NCEP), the gridded precipitation data by the PRISM Climate Group, Oregon State University, and the SCRAM (Support Center for Regulatory Atmospheric Modeling) Surface Meteorological Archived Data by the US Environmental Protection Agency (EPA). We thank the entities providing these resources for this project.

We would also like to acknowledge the contributions of Trihydro (Mr. Brian Robson and Mr. Jim Vanderweide), WYDOT Planning (Ms. Enid White), WYDOT Winter Research (Ms. Kathy Ahlenius) for their input, help, and advice.

## References


Curtis, J. and Kate Grimes (2004) *Wyoming Climate Atlas*. Wyoming Water Development Commission, Cheyenne, WY. 328p.

Johnson R.J. (2015) *Long-term Energy-balance Modeling of Interannual Snow and Ice in Wyoming using the Dynamic Equilibrium Concept*, M.S. Thesis, Department of Civil and Architectural Engineering, University of Wyoming, Laramie, Wyoming, pp. 106.

Heward, J. R. (2015). *The Effects of a Changing Landscape on Snow Accumulation and Ablation in the Upper Little Laramie River Wyoming Watershed*. M.S. Thesis, Department of Civil and Architectural Engineering, University of Wyoming, Laramie, Wyoming, pp. 106.

Hong, S. Y., & Lim, J. O. J. (2006). The WRF single-moment 6-class microphysics scheme (WSM6). J. Korean Meteor. Soc, 42(2), 129-151.

Leung, L. R., Y.-H. Kuo, and J. Tribbia (2006). Research Needs and Directions of Regional Climate Modeling Using WRF and CCSM. *Bulletin of the American Meteorological Society*, **87,** 1747-1751.

Lynch, P. (2008). The origins of computer weather prediction and climate modeling. *Journal of Computational Physics* (University of Miami) 227 (7): 3431–44.

Mesinger, F., G. DiMego, E. Kalnay, K. Mitchell, and Coauthors, (2006) North American Regional Reanalysis. Bulletin of the American Meteorological Society, 87, 343–360, doi:10.1175/BAMS-87-3-343.

Mewes, J. J. (2011). *Mapping weather severity zones* (No. CR10-02).

Morrison, H., & Gettelman, A. (2008). A new two-moment bulk stratiform cloud microphysics scheme in the Community Atmosphere Model, version 3 (CAM3). Part I: Description and numerical tests. Journal of Climate, 21(15), 3642-3659.

Nakicenovic, N., & Swart, R. (2000). Special report on emissions scenarios. Special Report on Emissions Scenarios, Edited by Nebojsa Nakicenovic and Robert Swart, pp. 612. ISBN 0521804930. Cambridge, UK: Cambridge University Press, July 2000., 1.

Hartmann, D.L., A.M.G. Klein Tank, M. Rusticucci, L.V. Alexander, S. Brönnimann, Y. Charabi, F.J. Dentener, E.J. Dlugokencky, D.R. Easterling, A. Kaplan, B.J. Soden, P.W. Thorne, M. Wild and P.M. Zhai, 2013: Observations: Atmosphere and Surface. In: Climate Change 2013: The Physical Science Basis. Contribution of Working Group I to the Fifth Assessment Report of the Intergovernmental Panel on Climate Change [Stocker, T.F., D. Qin, G.-K. Plattner, M. Tignor, S.K. Allen, J. Boschung, A. Nauels, Y. Xia, V. Bex and P.M. Midgley (eds.)]. Cambridge University Press, Cambridge, United Kingdom and New York, NY, USA.

Kusaka, H, H Kondo, Y Kikegawa, F Kimura (2001) A simple single-layer urban canopy model for atmospheric models: comparison with multi-layer and slab models, Boundary-Layer Meteorology 101 (3), 329-358.

Tabler, R. D. (1988). *Snow fence handbook* (Release 1.1). Tabler & Associates, Laramie, Wyoming. 169 pp.

Tabler, R. D. (1991). Improved guidelines for snow fences. *Proceedings, Strategic Highway Research Program Products, ASCE Highway Division* (8-10 April 1991; Denver, Colorado), 79 pp.

Tabler, R. D. (1991). Snow Fence Guide. National Research Council, Washington, D.C., 61 pp.

Tabler, R.D. (1994). Design Guidelines for the Control of Blowing and Drifting Snow. Strategic Highway Research Program, Publication SHRP-H-381, National Research Council, Washington, D.C. 364 pp.

Tabler R.D. (2003). Controlling Blowing and Drifting Snow with Snow Fences and Road Design. Final Report NCHRP Project 20-7 (147) Tabler & Associates, Laramie, Wyoming. 345 pp.

Tabler, R.D. (2006). Three-Dimensional Roughness Elements for Snow Retention. WYDOT FHWA-WY-06/04F.

Tabler, R.D. and J. Meena (2006). Effects of Snow Fences on Crashes and Road Closures – A 34-Year Study on Wyoming Interstate 80. *Proceedings for the 13th International Conference on Cold Regions Engineering*. ASCE.

Tabler, R.D. (2009) *Snow Snake Performance Monitoring*. WYDOT FHWA-WY-09/01F.

Skamarock, W. C., J. B. Klemp, J. Dudhia, D. O. Gill, D. D. M. Barker, M. G. Duda, X.-Y. Huang, W. Wang, and J. G. Powers (2008). *A description of the advanced research WRF version 3*, Tech. Note NCAR/TN-475+STR, Natl. Cent. for Atmos. Res., Boulder, Colo.

WYDOT. (2009). *Importance of Snow Fence*. Brochure from WYDOT Winter Research Services.

Saucier, W. J. (2003). Principles of Meteorological Analysis. Courier Dover Publications. ISBN 978-0-486-49541-5

Vautard et al., 2010

Yamartino, R. J. (1984). A comparison of several "single-pass" estimators of the standard deviation of wind direction. Journal of Climate and Applied Meteorology, 23(9), 1362-1366.